„ISOBAR EXCITATIONS AND LOW ENERGY SPECTRA OF LIGHT NUCLEI“

„Isobare Anregungen und tiefliegende Energiespektren leichter Kerne“

Dissertation

zur Erlangung des Grades eines Doktors der Naturwissenschaften

der Fakultät für Physik der Eberhard-Karls-Universität zu Tübingen

vorgelegt von

Piotr Czerski

aus Krakow

1984

„ISOBAR EXCITATIONS AND LOW ENERGY SPECTRA OF LIGHT NUCLEI“

„Isobare Anregungen und tiefliegende Energiespektren leichter Kerne“

Dissertation

zur Erlangung des Grades eines Doktors der Naturwissenschaften

der Fakultät für Physik
der Eberhard-Karls-Universität zu Tübingen

vorgelegt von

Piotr Czerski
aus Krakow

1984

Tag der mündlichen Prüfung:	30 July 1984
Dekan	Prof. Dr. K.-H. Herrmann
1. Berichterstatter:	Prof. Dr. Amand Faessler
2. Berichterstatter:	Prof. Dr. Herbert Müther

Offsetdruck Spengler
Lessingstraße 4 · 7401 Neustetten 1
Telefon (0 74 72) 2 21 45

Für Bożena

Digitized by the Internet Archive
in 2026

https://archive.org/details/IA41547612_0041

ABSTRACT

CZERSKI, PIOTR

ISOBAR EXCITATIONS AND LOW ENERGY SPECTRA OF LIGHT NUCLEI

The aim of this investigation is to study the possible influence of inner excitations of nucleons into the $\Delta(3,3)$-resonance on the low lying spectra of light nuclei like ^{12}C and ^{16}O. Before we can study the effect of such exotic configurations one has to perform a reliable investigation within the normal nuclear model, which is based on a microscopic theory. This is achieved by performing RPA (Random Phase Approximation) calculations using a realistic residual interaction derived from the Brueckner G-matrix. An efficient parametrisation of the residual interaction is introduced and the reliability of the more phenomenological parametrisations which are generally used is discussed. Within such realistic calculations, the isobar effects are small.

ISOBARE ANREGUNGEN UND TIEFLIEGENDE ENERGIESPEKTREN LEICHTER KERNE

Das Ziel dieser Rechnungen ist das Studium möglicher Einflüsse innerer Anregungen von Nukleonen, insbesondere der $\Delta(3,3)$-Resonanz auf tiefliegende Zustände leichter Kerne wie ^{12}C und ^{16}O. Bevor wir die Effekte bei solch exotischen Konfigurationen studieren können, müssen wir zuverlässige Rechnungen für übliche, auf einer mikroskopischen Theorie beruhende, Kernmodelle durchführen. Dies kann durch eine RPA (Random Phase Approximation) Rechnung erreicht werden, die mit einer realistischen Restwechselwirkung durchgeführt wird. Diese Restwechselwirkung wird aus der Brücknerschen G-Matrix berechnet. Für die Restwechselwirkung wird eine Parametrisierung eingeführt, die es erlaubt die Wechselwirkung, in effizienter Weise zu berechnen. Die Zuverlässigkeit der sonst üblichen phänomenologischen Parametrisierungen wird diskutiert. Bei einer realistischen Rechnung sind die Effekte der Isobar-Anregungen klein.

CONTENTS

1. INTRODUCTION 1

2. DETAILS OF CALCULATIONS

2.1 RPA calculations 4

2.2 The Residual Intaraction 7

2.3 The Single Particle Basis and the Configuration Space 14

2.4 Coupling to the Electromagnetic Field 19

3. COMPARISION BETWEEN THE LOCAL FORCE AND THE ^{16}O G-MATRIX 22

4. SPIN-ISOSPIN EXCITATIONS COMPARISION BETWEEN FINIT NUCLEI AND NUCLEAR MATTER 34

5. INFLUENCE OF THE Δ-ISOBARS ON THE NUCLEAR STRUCTURE AND MAGNETIC TRANSITIONS IN LIGHT NUCLEI ^{12}C AND ^{16}O

5.1 Introduction 44

5.2 Discussion and Results 46

6. CONCLUSIONS 53

APPENDICES

A Calculation of the Matrix Elements of the G-operator 55

B Single Particle Matrix Element for the Magnetic Form Factor 61

C Calculation of the Radial Matrix Element 66

D Useful Mathematical Formulae 69

REFERENCES 71

FIGURE CAPTIONS 77

TABLES 80

FIGURES 96

1. INTRODUCTION

In the conventional model of nuclear structure investigations an atomic nucleus is considered as a system of inert nucleons, which interact by a instantaneous two-body force and can be described in the framework of non-relativistic quantum mechanics. For microscopic nuclear structure calculations within this model one has to solve two problems which are almost independent from each other. In a first step one has to determine the interaction between the nucleons. For really microscopic investigations the nucleon-nucleon (NN) interaction is determined by an analysis of the two-nucleon data, which are the NN phase shifts and the data of the deuteron. This can be done e.g. by considering a purely phenomenological ansatz to fit the NN data (see e.g. [1-3]). An alternative way is to consider the meson exchange model for the NN interaction and to describe the NN force by a One-Boson-Exchange-Potential (OBEP) (see [4],[5]). Also in this model some parameters have to be adjusted to obtain a quantitative fit of the NN phase shifts. One then uses this NN potential for the two-body part of the nuclear hamiltonian, adds the kinetic energy for the relative motion of the nucleons and tries to solve the Schrödinger equation for this nuclear many-body problem. Some of the general assumptions underlying this procedure may be summarized as follows:

-two nucleons in the medium of a nucleus feel the same NN interaction as in the vacum of NN scattering

-the effect of three- or other many-nucleon forces can be neglected

-for nuclear structure calculations the nucleons can be regarded as inert particles which do not exhibit any inner structure

Now one topic of this thesis is the discussion of the question: to which extend may inner excitations of the nucleon, influence the excitation spectra and other spectroscopic properties of nuclei. For the inner excitations of the nucleon we will restrict the discussion to the $\Delta(3,3)$ resonance at 1232MeV. However, before one may answer the question on the importance of isobar degrees of freedom, one must try to perform a realistic microscopic nuclear structure calculation, which considers the conventional nucleonic degrees of freedom only. We will limit the discussion to the excitation spectrum of doubly closed shell nuclei like ^{16}O. For a description of these nuclei the Random Phase Approximation (RPA) has been used with large success. The same technique will be used here (for details see Chapter 2.1). In order to perform real microscopic calculations we will not consider phenomenological residual interactions, as it has usually been done but start from a realistic OBE potential. In order to take into account the effects of the strong short range components one has to renormalize such a realistic potential by solving the Bethe-Goldstone equation, which leads to the Brueckner G-matrix. A very efficient way of evaluating such G-matrix elements has been developed and is described in Chapter 2.3 of this thesis. The rest of Chapter 2 gives an

overview of the methods used to perform structure calculations in nuclei with inclusion of the Δ resonance.

In Chapter 3 we compare the G-matrix obtained from the solution of the Bethe-Goldstone equation for the finite nuclei and the given nucleon-nucleon bare interaction with our effective local interaction determined for the same bare interaction. The comparision is done using the RPA calculations for excited states of ^{16}O. In Chapter 4 we discuss the effective G-matrix and compare it with the commonly used approximation for the residual particle-hole interaction containing π and ρ-exchange plus a repulsive constant g'. Finally, in Chapter 5 we show the influence of the Δ-isobar degrees of freedom on the low-lying excitation spectra, magnetic transition probabilities and form factors in ^{16}O and ^{12}C.

All important analytical details of the calculations are summarized in appendices.

2. DETAILS OF CALCULATIONS

2.1 RPA CALCULATIONS

A main topic of this thesis is to study the effect of the high-lying particle-hole (Δ-hole) excitations on the low energy nuclear structure observables. These include energies and electromagnetic transition probabilities and form factors. A consistent study of high- and low-lying ph configurations can be performed in the framework of the Random Phase Approximation.

The RPA is supposed to give a good description for nuclei which in zero order approximation can be regarded as doubly closed (^{16}O, ^{40}Ca, ^{48}Ca, ^{56}Ni, ^{132}Sn, ^{208}Pb). In this thesis light nuclei are investigated to establish the usefulness of realistic interactions as discussed in Chapter 2.2. Therefore the nucleus ^{16}O will be the main object of study. Since also ^{12}C has been discussed very often in the literature in conection with virtual isobar degrees of freedom, the RPA is also applied to the unnatural parity states in ^{12}C. For such states the complicated nature of the ground state might be of somewhat less influence then for the natural parity states.

In the conventional RPA one approximates the excited (collective) states as a superposition of particle-hole pairs acting on the ground state $|0\rangle$ of a given nucleus

$$|n\rangle = \sum_{ph} \left[X^n_{ph} a^\dagger_p a_h - Y^n_{ph} a^\dagger_h a_p \right] |0\rangle, \qquad (2.1.1)$$

where p and h denote single-particle states above and below Fermi surface, respectively. The amplitudes X and Y are given by the well known RPA equation

$$\begin{pmatrix} A & B \\ B^* & A^* \end{pmatrix} \begin{pmatrix} X \\ Y \end{pmatrix} = E \begin{pmatrix} X \\ -Y \end{pmatrix} \qquad (2.1.2)$$

where the matrices A and B are real in this case and given by

$$A = \langle p_1 h_1 \mid G \mid p_2 h_2 \rangle + \delta_{p_1 p_2} \delta_{h_1 h_2} (E_p - E_h) \ , \qquad (2.1.3a)$$

$$B = \langle p_1 h_1 \overline{(p_2 h_2)} \mid G \mid 0 \rangle \ . \qquad (2.1.3b)$$

E_p and E_h denote the single-particle energies for particles and holes respectively. The eigenvectors of this eigenvalue problem satisfy orthonormality relations

$$\sum_{ph} (X^k_{ph} X^l_{ph} - Y^k_{ph} Y^l_{ph}) = \delta_{kl} \quad , \quad (E_l > 0) \ . \qquad (2.1.4)$$

To calculate transition probabilities between the excited state $|n\rangle$ and the ground states $|0\rangle$ we have for the one-body operator Q the following expresion:

$$\langle n | Q | 0 \rangle = \sum_{ph} (X^n_{ph} + Y^n_{ph}) \, Q_{ph} \ , \qquad (2.1.5)$$

where Q_{ph} denotes the single-particle matrix element of Q.

This formalism can easily be extended to include Δ isobars in the calculation. In doing this one treats the Δ iso-

bars as an elementary particle in the many body system. The structure of the RPA matrices with inclusion of isobar particle states is shown diagramaticaly in Fig.1. In Fig.1a the "A-matrix", leaving out the diagonal terms containing the single-particle energies is displayed. The dashed line represents in those cases where a Δ-isobar is attached to the vertex the isovector mesons π and ρ (as discussed in Chapter 2.2). In the pure nucleonic case short-range calculations have been included and the dashed line represents the full G-matrix interaction. Also explicitly the exchange terms are shown which are considered here. In Fig.1b the backward going "B matrix" are shown. In addition short-range correlations for 2Δ-2h excitations must be taken into account (see Chapter 2.2), these contributions modify the lower right corner of the new "B-matrix".

In order to solve the RPA equation (2.1.2) we need the single-particle wave functions, the single-particle energies and the matrix elements of the residual interaction calculated in the basis of the single-particle wave functions. As far as possible we take the single-particle energies from experiment. For the other cases, high-lying resonances and deep-lying holes, we use the solutions of the Woods-Saxon potential (details are discussed in Chapter 2.3) used to generate the single-particle basis. "Experimental" single-particle energies, for three major shells, are displayed for ^{16}O and ^{12}C in Figs 2a and 2b, respectively. Since we are interested only in the low-lying states in ^{16}O and ^{12}C the influence of the choice of single-particle energies for high-lying configurations is small. Due to coherence effects these high-lying states can make a substantial contribution

to the transition probabilities and even to the excitation energies of low-lying collective states. The dimension of the model space is found by testing the convergence of the RPA results and is discussed in Chapter 5.

2.2 THE RESIDUAL INTERACTION

The effective ph-interaction used in the RPA calculations is based on Brueckner's reaction matrix (G-matrix). Different approximations of G which will be explained below were used. The bare interaction which is refered to as HEA-potential [6], [7] is based on the one boson exchange picture for the nucleon-nucleon (NN) interaction which is very succesful in reproducing the NN scattering data. One of the purposes of this work is to establish the usefulness of the G-matrix as a ph-interaction. Therefore it is necessary to do RPA calculations in a large model space with corresponding realistic wave functions. In order to keep the numerical effort of such calculation in reasonable limits it is useful to have a simple yet accurate representation of the G-matrix which allows the calculation of the matrix elements in an arbitrary basis. In Chapter 3 of this thesis it will be demonstrated that it is possible to represent this interaction sufficiently accurate by a local form which was proposed in [8]. This local form of the G-matrix is obtained from a nuclear matter calculation of the G-matrix. The integral equation, Bethe-Goldstone equation, for the G-operator reads

$$G(E) = V + V \frac{Q}{E - H_o} G(E) \ , \qquad (2.2.1)$$

where V is the bare interaction, the HEA meson exchange potential, Q is the Pauli operator, E is the starting energy and H_o is the energy operator for the intermediate particle states. In shorter notation we can rewrite eq.(2.2.1) as

$$G = V + \tilde{G} \ . \qquad (2.2.2)$$

Now the G-matrix plays the same role for the interaction of two nucleons in the nuclear medium as the T-matrix, the solution of the Lipmann-Schwinger equation, for the vacuum. This means that G as well as T accounts for multiple scattering processes and therefore the difference $G-V=\tilde{G}$ in eq,(2.2.2) mainly accounts for the short-range correlations in the two-nucleon wave functions. For the multiple scattering processes contained in G only those intermediate states are allowed which are not occupied by other nucleon. This effect of the Pauli principle is reflected by the Pauli operator Q in eq.(2.2.1).

In [8] it is shown that is very well possible to describe the short-range correlations effects contained in G by simple "effective" meson exchange potentials. These mesons are understood in such a way that they represent the different symmetries of the interaction. For example for the central part of the interaction the following invariant operators are choosen

$$1,\ \sigma_1\cdot\sigma_2,\ \tau_1\cdot\tau_2,\ \sigma_1\cdot\sigma_2\tau_1\cdot\tau_2 \qquad (2.2.3a)$$

and for the tensor part

$$S_{12}(\hat{q}),\ S_{12}(\hat{q})\ \tau_1\cdot\tau_2, \qquad (2.2.3b)$$

where σ and τ are spin and isospin pauli matrices and $S_{12}(\hat{q})$ is the tensor operator

$$S_{12}(\hat{q}) = 3\ \sigma_1\cdot\hat{q}\ \sigma_2\cdot\hat{q} - \sigma_1\cdot\sigma_2\ . \qquad (2.2.4)$$

In this work the representation of G in terms of Yukawa functions obtained in [8] for nuclear matter with the Fermi momentum $k_F=1.2\text{fm}^{-1}$ was used. The force is denoted by G^I_{NM} here and was obtained for an average starting energy relevant for nuclear matter of this density of E=-74.0 MeV. The parameters of $\tilde{G}$ for this force are given in Table 1. For the complete representation of G one needs in addition a local parametrisation of the bare HEA potential V. The parameters of this local equivalent potential were obtained in the same way as for $\tilde{G}$ (see [8]). Note that due to the local nature of this force no two-body spin-orbit force is contained in the calculations. The parameters of this local approximation of the bare potential are given in Table 2. Note that in this case linear combinations of the invariants $\sigma_1\cdot\sigma_2$ and $S_{12}(\hat{q})$ are used. For this case we use the relations

$$\sigma_1\cdot q\ \sigma_2\cdot q = 1/3\ \sigma_1\cdot\sigma_2 q^2 + 1/3\ S_{12}(\hat{q})q^2\ , \qquad (2.2.5)$$

$$\sigma_1 x\mathbf{q}\ \sigma_2 x\mathbf{q} = 2/3\ \sigma_1\cdot\sigma_2 q^2 - 1/3\ S_{12}(\hat{\mathbf{q}})q^2\ . \qquad (2.2.6)$$

With the choice of invariant operators (2.2.3) we are able to study the central and tensor part of the force seperatly. For the momentum dependence of the central components we assume the form

$$\frac{A}{m^2 + k^2}\cdot \text{spin-isospin operators}\ , \qquad (2.2.7a)$$

which is motivated by the meson exchange picture. For the tensor parts

$$\frac{A}{m^2}\frac{q^2}{m^2 + q^2}\ S_{12}(\hat{\mathbf{q}})\cdot\text{isospin operator}\ , \qquad (2.2.7b)$$

is used. In order to test the dependence of the G matrix on the density of the nuclear matter and the starting energy, the Bethe-Goldstone equation has also been solved for $k_F = 1.06\,\text{fm}^{-1}$ (a density which is close to the average density in ^{16}O) and a starting energy E=-20MeV (which is a reasonable avarage for performing ph-calculations). This force is denoted by G^{II}_{NM} and its parameters can be found in Table 3. The calculation of the ph matrix elements in an oscillator basis is described in Appendix A. The method of [9] was choosen since this allows for a detailed understanding of the matrix elements in terms of the momentum dependence of the force.

If one now wants to investigate the influence of $\Delta(1232)$ isobars on the excitation spectrum of nuclei, one has to

consider also a form for the interaction which couples the Δ-particle nucleon-hole states (Δh) to the conventional ph states and a residual interaction between the Δh states. In the meson exchange picture only π and ρ-mesons can couple the spin and isospin of the nucleon and the isobar therefore only π and ρ-exchange transition potentials from ph to Δh states have to be considered. This Δ-isobar nucleon-hole (Δh) ph interaction takes the same Yukawa form as discussed above and explicitly reads

$$V_{N\Delta}(q) = -\frac{f_\pi f_\pi^*}{m_\pi^2}\,\frac{1}{m_\pi^2 + q^2}\,\sigma_1\cdot q\; S_2\cdot q\;\tau_1\cdot T_2 \qquad (2.2.8)$$

$$-\frac{f_\rho f_\rho^*}{m_\rho^2}\,\frac{1}{m_\rho^2 + q^2}\,\sigma_1 x q\cdot S_2 x q\;\tau_1\cdot T_2\ ,$$

where f_π and f_ρ are pion and rho coupling constants in the NNπ and NNρ vertices. For NΔπ and NΔρ vertices we use the following coupling constants

$$f_\pi^* = 2f_\pi\ , \qquad (2.2.9a)$$

$$f_\rho^* = 2f_\rho \qquad (2.2.9b)$$

as suggested by the static Chew-Low model. S is the operator which creates spin 3/2 from a spin 1/2 state, the so called transition spin (see [10]). The reduced matrix elements are defined as

$$\langle 3/2 \| S \| 1/2 \rangle = - \langle 3/2 \| S^{+} \| 1/2 \rangle = 2 \; ; \qquad (2.2.10)$$

analogous expressions hold for the isospin operators T and T^{+}.

The Δh interaction which is used in this work has two components corresponding to a forward and backward going interaction. The forward going term which connects a Δh-state with a Δh-state is

$$V^{F}_{\Delta\Delta} = - \frac{f_\pi^{*} f_\pi^{*}}{m_\pi^{2}} \frac{1}{m_\pi^{2} + q^{2}} S_1 \cdot q \; S_2^{+} \cdot q \; T_1 \cdot T_2^{+} \qquad (2.2.11)$$

$$- \frac{f_\rho^{*} f_\rho^{*}}{m_\rho^{2}} \frac{1}{m_\rho^{2} + q^{2}} S_1 x q \cdot S_2^{+} x q \; T_1 \cdot T_2^{+} \; ,$$

where as the backward term recives contribution from

$$V^{B}_{\Delta\Delta} = - \frac{f_\pi^{*} f_\pi^{*}}{m_\pi^{2}} \frac{1}{m_\pi^{2} + q^{2}} S_1 \cdot q \; S_2 \cdot q \; T_1 \cdot T_2 \qquad (2.2.12)$$

$$- \frac{f_\rho^{*} f_\rho^{*}}{m_\rho^{2}} \frac{1}{m_\rho^{2} + q^{2}} S_1 x q \; S_2 x q \; T_1 \cdot T_2 \; .$$

At this point one should note that no exchange contribution of (2.2.11-2.2.12) are calculated, in contrast to all other parts of the interaction, because this would require the knowledge of $\Delta\Delta\pi$ and $\Delta\Delta\rho$ vertices and also those for the other mesons (see also Chapter 2.1 and Fig.1).

Short range correlations do not influence the transition potential very much. This can be quite easily understood

from the partial wave expansion of the interaction the $NN \longrightarrow N\Delta$ in the particle-particle representation. Due to the spins and isospins of the baryons there are no interaction channels leading from S-channel (orbital momentum of the relative motion) to S-channel. Since therefore the effect of short range correlations is negligible for the transition potential $NN \longrightarrow N\Delta$ no additional short-range correlations in the form of $g'_{N\Delta}\ \sigma_1 \cdot S_2\ \tau_1 \cdot T_2$ are considered in this thesis. Since there are short-range contributions to the Δh-Δh interactions we simulate these by a parameter $g'_{\Delta\Delta}$ so that we obtain the following G-matrix like transition potentials

$$G_{N\Delta} = V_{N\Delta} \ ,$$

$$G_{\Delta\Delta} = V^F_{\Delta\Delta} + V^B_{\Delta\Delta} +$$

$$+ g'_{\Delta\Delta} \frac{f_\pi^* f_\pi^*}{m_\pi^2} \left(S_1 \cdot S_2\ T_1 \cdot T_2 + S_1 \cdot S_2^+\ T_1 \cdot T_2^+ \right) , \qquad (2.2.13)$$

where for $g'_{\Delta\Delta}$ part only direct matrixelemants are calculated. The $V_{N\Delta}$ or $V_{\Delta\Delta}$ interaction we can rewrite in such a form so as to obtain a separation between central V^C and tensor V^t parts. For the π-exchange only we have

$$V^C_{N\Delta} = \frac{1}{3} \frac{f_\pi f_\pi^*}{m_\pi^2} \frac{q^2}{m_\pi^2 + q^2} \sigma_1 \cdot S_2\ \tau_1 \cdot T_2 \ , \qquad (2.2.14)$$

$$V^t_{N\Delta} = \frac{1}{3} \frac{f_\pi f_\pi^*}{m_\pi^2} \frac{q^2}{m_\pi^2 + q^2} S_{12}(\hat{q})\ \tau_1 \cdot T_2 \ . \qquad (2.2.15)$$

The hole $V_{N\Delta}$ interaction is equal to the sum of central and tensor part. To derive formulas (2.2.14-2.15) we used the following relations

$$\sigma_1 \cdot \mathbf{q}\ \mathbf{S}_2 \cdot \mathbf{q} = 1/3\ \sigma_1 \cdot \mathbf{S}_2 q^2 + 1/3\ S_{12}(\hat{\mathbf{q}}) q^2 \ , \qquad (2.2.16)$$

$$\sigma_1 \mathrm{x} \mathbf{q}\ \mathbf{S}_2 \mathrm{x} \mathbf{q} = 2/3\ \sigma_1 \cdot \mathbf{S}_2 q^2 - 1/3\ S_{12}(\hat{\mathbf{q}}) q^2 \ . \qquad (2.2.17)$$

$S_{12}(\hat{q})$ is given by (2.2.4), applied to the spin transition matrices **S.** spin matrices.

2.3 THE SINGLE PARTICLE BASIS AND THE CONFIGURATION SPACE.

To carry out the RPA calculations we need the single-particle basis and energies of the nucleus under consideration. A realistic description of the mean field of the nucleus is provided by potentials of Woods-Saxon type. In order to get the single particle spectrum and the corresponding wave functions one therefore has to solve the Schrödinger equation

$$\left(-\frac{\hbar^2}{2\mu} \Delta + V_{WS}(r) \right) | nljm \rangle_{WS} = E | nljm \rangle_{WS} \qquad (2.3.1)$$

with the reduced mass

$$\mu = m\left(\frac{A-1}{A} \right), \quad [\, m - \text{nucleon mass, } A - \text{mass number}\,] \qquad (2.3.2)$$

and the Woods-Saxon potential of the form

$$V_{WS} = V_o \left[1+\exp((r-R)/a) \right]^{-1} + V_c(r) \qquad (2.3.3)$$

$$+ V_{LS}\left(\frac{\hbar}{m_\pi c}\right)^2 \frac{1}{r}\frac{d}{dr}\left[1+\exp((r-R_{LS})/a_{LS})\right]^{-1} \mathbf{L}\cdot\mathbf{S} ,$$

where m_π is the pion mass (m_π=138.5MeV).

The choice of the parameters was done in such a way as to obtain reasonable agreement between the eigenvalues of eq.(2.3.1) and the experimental energies near the Fermi surface. All parameters are displayed in Table 1a for ^{12}C and in Table 1b for ^{16}O. The Coulomb potential of a uniform charge distribution with a radius R_c (R_c=1.25$A^{1/3}$) is used:

$$V_c(r) = \begin{cases} \dfrac{e^2 Z}{r} & r<R_c \\ \dfrac{e^2 Z}{R_c}\left(\dfrac{3}{2}+\dfrac{1}{2}\left(\dfrac{r}{R_c}\right)^2\right) & r>R_c \end{cases} \qquad (2.3.4)$$

For the bound states, E<0 we expand the Woods-Saxon wave function in terms of the harmonic oscillator wave funtions:

$$|nljm\rangle_{WS} = \sum_{n'} c_{n'} |n'ljm\rangle_{HO} , \qquad (2.3.5)$$

where summation goes up to the eight expansion coefficients [11]. After substitution of eq.(2.3.5) into eq.(2.3.1) and after multiplication from the left hand side by $\langle nljm|_{HO}$ we have

$$\sum_k (T_{n,k} + \langle nljm| V_{WS} |kljm\rangle_{HO})c_k = Ec_n\delta_{nk} , \qquad (2.3.6)$$

where $T_{n,k}$ is the matrix element of the kinetic energy operator between harmonic oscillator states

$$T_{n,k} = \begin{cases} \frac{\hbar\omega}{2}(2n+1-1/2), & \text{for } k=n \\ \frac{\hbar\omega}{2}[n(n+1+1/2)]^{1/2}, & \text{for } k=n+1 \\ 0, & \text{otherwise} \end{cases} \qquad (2.3.7)$$

The solution of eq.(2.3.6) gives a set of expansion coefficients for each Woods-Saxon eigenstate.

For unbounded (scattering) states, E>0 we solve the Schrödinger equation for the radial wave function [12].

$$\frac{d^2}{dr^2} u_{lj}(r,k) + [k^2 - \frac{l(l+1)}{r} - V_{WS}] u_{lj}(r,k)=0 , \qquad (2.3.8)$$

where $k^2=(2\mu/\hbar^2)E$.

Since in the actual calculation of matrix elements of the interaction there are always bound wave functions involved, one actually needs the scattering waves only in the overlap region with the bound wave functions supplemented by a distance which is related to the range of the interaction. Therefore one can discretize these wave functions in this relevant volume and expand again in harmonic oscillator waves. For ^{12}C and ^{16}O the radius of this sphere was taken to be 6fm. As a prescription to obtain the discretized energy states we choose the energies for which the scattering wave show a resonance i.e. for which $\sin^2\delta_l$ has a maximum, where δ_l is the scattering phase shift. We expand such a solution in the harmonic oscilatior basis. To obtain a set of basis states with quantum numbers εljm we proceed in the following way. In case there is already a bound wave function with the same quantum numbers one must orthonormalize the first reso-

nance one finds onto this state. The next resonance must then be constructed orthonormal with respect to the first two states etc. This expanded wave function is orthonormalized with the Schmidt method using the recursion formula

$$|\Psi_N\rangle = N(|\Phi_N\rangle - \sum_{m=1}^{N-1} |\Psi_m\rangle\langle\Psi_m|\Phi_N\rangle) \ , \tag{2.3.9}$$

where $|\Psi_N\rangle$ is the ortonormalized wave function. This procedure starts with N=1. The $(|\Phi_N\rangle)$ is simply the set of orthonormal states of the form

$$\begin{aligned} |\Phi_1\rangle &= (1,0,0,0,\ldots) \\ |\Phi_2\rangle &= (0,1,0,0,\ldots) \\ |\Phi_3\rangle &= (0,0,1,0,\ldots) \\ &\ldots \end{aligned} \tag{2.3.10}$$

in oscillator space.

In the calculations we used the following harmonic oscilator constants

$$\hbar\omega = 41.5(A-1)^{1/3} \ , \tag{2.3.11}$$

$$b^2 = \frac{\hbar}{\mu\omega} = \frac{1}{\hbar\omega}\frac{A}{A-1}\left[6.44\right]^2 \ .$$

To obtain now e.g. matrix elements of the two-body interaction in this basis one calculates

$$\langle n_1, n_2^{-1} \mid V \mid n_3, n_4^{-1} \rangle_{WS} = \sum_{i_1 i_2 i_3 i_4} c_{i_1} c_{i_2} c_{i_3} c_{i_4} \langle i_1, i_2^{-1} \mid V \mid i_3, i_4^{-1} \rangle_{HO} , \qquad (2.3.12)$$

where c_i are expansion coefficients eq.(2.3.5). In eq.(2.3.12) only n quantum numbers are displayed because the other ones (l,j) remain unchanged after expansion. The harmonic oscillator matrix elements of the interaction are calculated in Appendix A.

A short discussion of the wave functions obtained in this way will now be given. In Fig.3 and Fig.4 the wave functions of the Woods-Saxon state are plotted in the r space. In Fig.3 the wave functions for the bound proton and neutron $p_{3/2}$ state in ^{16}O are displayed. In Fig.4 the first unbound $p_{3/2}$ neutron and $f_{7/2}$ proton states are shown. All curves are calculated for ^{16}O with the harmonic oscillator parameter b=1.639fm. The first three curves in each Figure are solutions of the the Schrödinger equation (2.3.1). The fourth, dash-dotted one, is the corresponding harmonic oscillator wave function with b=1.639fm. The solid line with the name "scatt" represents a solution obtained for the Woods-Saxon potential for unbounded states at resonance as described above. The dashed line "diag" is a solution with the first method used for the bounded states in Fig.4 also shown for unbound states. The dotted curve called "Speth" is a solution for the same potential but with the different method described in [13]. These wave functions were used in the RPA calculations done by Speth et al. [14] and the expansion coefficients were kindly placed to our disposal by the group in Jülich. The difference between the proton and

the neutron wave functions is due to the Coulomb potential for charged particles and to the different depth of the nuclear potential.

In our understanding the main difference between the wave function used by the group in Jülich and our wave function is related to the choice for the reduced mass. For the correct solution of the three dimensional collision process in the center-of-mass system e.g., the scattering in which a particle that has the reduced mass $\mu=m_1m_2/(m_1+m_2)$ colides with a fixed scattering center, it is necessery to use the reduced mass parameter consistently in the whole calculation starting from the Schrödinger equation (2.3.1) in contrast to the calculation of Speth et al.. In our case $m_1=m$ and $m_2=(A-1)m$ where m is a nucleon mass. In Fig.3 we plot wave functions for the bound states. All curves are more or less close to each other. One can already see some differences which are more pronounced for the scattering states. In Fig.4 we have two examples of sharp resonances. In both cases the so called "diag" wave function corresponds to the diagonalisation method for bound states. Of course this solution has no physical meaning and is plotted only to show the dangers of using such a wave function, it leads to unrealistic results. Specifically, for the scattering states one observes that the "Speth" wave functions are still very close to the harmonic oscillator one, whereas our solutions are more shifted outside the potential region.

2.4 COUPLING TO THE ELECTROMAGNETIC FIELD.

To study the electromagnetic properties of the excited nuclear states with inclusion of isobars, we have to consider the transition operator between isobar and nucleon states. Following [15], the gauge invariant operator $H_{N\Delta\gamma}$ can be written as

$$H_{N\Delta\gamma} = \bar{u}_\mu(p_\Delta, s_\Delta) \left[G_1 \left(\varepsilon^\mu - \frac{\varepsilon \cdot \gamma k^\mu}{m + M} \right) \gamma_5 \right.$$

$$\left. + G_2 \frac{p_N \cdot \varepsilon k^\mu - p_N \cdot k \varepsilon^\mu}{(m + M)^2} \gamma_5 \right] u(p_N, s_N) \,, \qquad (2.4.1)$$

where G_1 and G_2 are independent coupling constants, ε^μ is the polarization vector of the photon and u and u_μ represent the Dirac spinor for the nucleon and the Rarita-Schwinger spinor for the spin 3/2 particle, respectively. In our calculation the second term is omitted as a contribution of higher order relative to the first term.

After the nonrelativistic reduction of eq.(2.4.1) (for detailes see [16]) we have

$$H_{N\Delta\gamma} = G_1 \frac{eh}{2mc} \frac{m}{M} \mathbf{S} \cdot \mathrm{rot} \mathbf{A}\, T_3 \,, \qquad (2.4.2)$$

where m and M are nucleon and isobar masses, **A** is the vector potential of the electromagnetic field, **S** and **T** are generalizations of spin and isospin matrices, the reduced matrix elements are given by eq.(2.2.5).

After the multipole expansion of the vector potential **A** we end up in the long wave length limit with the magnetic transition operator

$$B(ML,\mu) = -\mu_N G_1 \frac{m}{M} \nabla(r^L Y_{Lm}(\hat{r})) \; S \; T_3, \qquad (2.4.3)$$

where L denotes the multipolarity of the transition.
The coupling constant G_1 is estimated from the multipole analysis of data on pion photoproduction on a free nucleon [17], [18].

$$G_1 = 1.3 g_p^s \, 2^{-1/2} = 5.14 \; , \qquad (2.4.4)$$

where g_p^s is the spin gyromagnetic factor for protons eq.(2.4.7). Adding to eq.(2.4.3) the standard magnetic transition operator for the nucleons, we have the expression for the full operator:

$$B(ML,\mu) = \mu_N \Big[\frac{2}{L+1} \nabla(r^L Y_{L\mu}(\hat{r}))\cdot L \; g^l + \nabla(r^L Y_{L\mu}(\hat{r}))\cdot s \; g^s$$

$$- G_1 \frac{m}{M} \nabla(r^L Y_{L\mu}(\hat{r}))\cdot S \; T_3 \Big] \; , \qquad (2.4.5)$$

where we use the following notation

$$g^s = \frac{1+\tau_3}{2} g_p^s + \frac{1-\tau_3}{2} g_n^s \; , \qquad (2.4.6a)$$

$$g^l = \frac{1+\tau_3}{2} g_p^l + \frac{1-\tau_3}{2} g_n^l \; , \qquad (2.4.6b)$$

$$\mu_N = \frac{e\hbar}{2mc} \quad \text{(nuclear magneton)} \; . \qquad (2.4.6c)$$

The spin (resp. orbital current) g-factor for the free proton (resp. neutron) are

$$g_p^s = 5.486, \qquad g_n^s = -3.826,$$
$$g_p^l = 1.0 \ , \qquad g_n^l = 0.0 \ . \tag{2.4.7}$$

For the electric transition we take then the operator in the long wave length limit to be

$$B(EL,\mu) = er^L \, Y_{L\mu}(\hat{r}) \, g^l \ , \tag{2.4.8}$$

where g^l id defined by eq.(2.4.6b).

3. COMPARISION BETWEEN THE LOCAL FORCE AND THE ^{16}O G-MATRIX.

Nuclear structure calculations using simple, phenomenological forces have been applied quite successfull in calculating nuclear properties all over the periodic Table [19]. The major advantage of using effective nucleon-nucleon (NN) interactions of simple structure is, that matrix elements are easily calculated for all kinds of nuclear structure model spaces. Furthermore the parameters of the interaction can be adjusted until agreement is obtained between the calculation and the experimental data. The main disadvantage of using such forces is due to the fact, that such investigations cannot be understood as real microscopic nuclear structure calculations since free parameters are ajusted. Therefore one would like to deduce the NN interaction to be used in nuclear structure calculations from a realistic NN potential, which has been fitted to the NN scattering data only. In order to account for those degrees of freedom, which are not treated explicitly in the nuclear structure calculation, one has to renormalize the bare NN interaction V. Typically the first step in this renormalization procedure is to evaluate the Brueckner G-matrix in order to pay attention to the short-range NN correlations. For some nuclear structure calculations, especially those performed in large model spaces, the G-matrix approximation might be sufficient, whereas in other cases,e.g. the standard example of shell-model calculations within the sd-shell, an additional renormalization might be needed [20]. However, in both cases one needs an efficient way for evaluating G-matrix elements in a reliable approximation. The exact solution of the Be-

the-Goldstone equation for finite nuclei is relatively complicated and is therefore a major obstacle for performing extensive calculations.

It is purpose of this Chapter to show that the effective interaction proposed in [8] provides such an approximation. This interaction is derived from the G-matrix calculated for nuclear matter. Since it is represented as a sum of local terms, it is quite easy to evaluate matrix elements. In order to obtain the G-matrix we have to solve the Bethe-Goldstone equation [21].

The Bethe-Goldstone equation which generates the two-body effective interaction reads in operator form

$$G(E) = V + V \frac{Q}{E-H_o} G(E) \tag{3.1}$$

A basic difference between this equation and the NN T-matrix consists in the presence of Pauli-Operator Q which forbids scattering of particles into states which are normally occupied. In nuclear matter this corresponds to states below the Fermi momentum k_F which is related to the density of nuclear matter by

$$\rho = \frac{2}{3\pi^2} k_F^2 \ . \tag{3.2}$$

In nuclear matter eq.(3.1) depends apart from the density dependence on two external parameters: the scatering energy E and the center of mass (c.m.) momentum of the interacting nucleons. In [8] the single-particle spectrum above the Fermi

momentum was described by the pure kinetic energy [22]. Since the c.m. momentum is not a good quantum number in a finite system and the dependence of G on it is rather weak, it is useful to solve eq.(3.1) only for one c.m. momentum which is taken to be the average c.m. momentum for two particles in the Fermi sphere [8]. Taking now a similar average starting energy one has to solve eq.(3.1) only once for a given density to obtain the nuclear matter G-matrix. For the correlation part of G which is denoted by G (see eq.2.2.2), one can obtain a local parametrization of the interaction which gives the same binding energy and Landau paramerers as the exact result (see [8]). In a similar way one can obtain a local representation of the bare interaction V. This means that one can summarize all the essential features of the G-matrix in nuclear matter in terms of simple local operators. In [8] the particle-hole (ph) representation was used to obtain these local operators (see also Chapter 2.2). Here we shortly repeat the arguments why this is a useful method.

If we assume the interaction to be local, this means that in momentum space the interaction only depends on the momentum transfer between two particles. Viewed differently, if two nucleons exchange a meson the interaction depends only on the momentum which the meson carries. Clearly mesons with different quantum numbers can be exchanged. In a ph-representation of the interaction (see Fig.5) these different mesons can be related to the quantum numbers of the ph state T, S, M to which they couple, where T is the total isospin, S the total spin and M the total spin projection on the direction of the momentum transfer $\mathbf{q}$ of the ph states. The converse is also true, e.g. for T=1, S=1, M=0 ph states

only the pion (or better pionic quantum numbers) can be exchanged. These considerations lead to the following ansatz for the local effective interaction operator

$$G(q;E,\rho) =$$

$$f'_{E,\rho}(q)\ \tau_1\cdot\tau_2 + g_{E,\rho}(q)\ \sigma_1\cdot\sigma_2 + g'_{E,\rho}(q)\ \sigma_1\cdot\sigma_2\ \tau_1\cdot\tau_2$$

$$+ h_{E,\rho}(q)\ S_{12}(\hat{q}) + h'_{E,\rho}(q)\ S_{12}(\hat{q})\ \tau_1\cdot\tau_2\quad \tau_1\cdot\tau_2\ , \qquad (3.3)$$

where $S_{12}(\hat{q})$ is given by eq.(2.2.4). Note that eq.(3.3) represenrs an operator which means that direct and exchange contributions (see Fig.5a and 5b) must be separately calculated. For the one pion exchange interaction e.g. only $g'_{E,\rho}(q)$ and $h'_{E,\rho}(q)$ survive which naturally do not depend on E and ρ and have the following form

$$g'_\pi(q) = h'_\pi(q) = \frac{1}{3}\frac{f_\pi^2}{m_\pi^2}\frac{k^2}{m_\pi^2+k^2}\ . \qquad (3.4)$$

What has been obtained by means of eq.(3.3) is the connection between the important momentum (q) dependence of the interaction and the spin isospin operators to which they belong (see eq.(3.4)). Clearly this is only important for finite range interactions like the one pion exchange. For zero-range (δ-force) interactions which are simply constant in momentum space, it is always possible to rearrange the distribution of strength among the various operators. To demonstrate this, let's assume we have found a parametrisation for the G-matrix in terms of f, f', g and g' (zero-range in-

teractions act only in relative s-waves and are therefore not relevant for the tensor components). Adding now δf, $\delta f'$, δg and $\delta g'$ δ-forces and requesting the same matrix elements as before leads to the following relations for different ph chanels [8]

$$3\delta f - 3\delta f' - 3\delta g - 9\delta g' = 0 \qquad (S=0,T=0)\ , \qquad (3.5a)$$

$$-\delta f + 5\delta f' - 3\delta g + 4\delta g' = 0 \qquad (S=0,T=1)\ , \qquad (3.5b)$$

$$-\delta f - 3\delta f' + 5\delta g + 3\delta g' = 0 \qquad (S=1,T=0)\ , \qquad (3.5c)$$

$$-\delta f + \delta f' + \delta g + 3\delta g' = 0 \qquad (S=1,T=1)\ . \qquad (3.5d)$$

Obviously eq.(3.5a) and eq.(3.5d) are equivalent. Substracting eq.(3.5d) from eq.(3.5b) and eq.(3.5c) one obtains the same equation:

$$4\delta f - 4\delta g = 0\ , \qquad (3.6)$$

which together with eq.(3.5d) represent only two restrictions for four quantities. Therefore it is clear that one can add a contstant in one channel and get equivalent results by adding constants in other channels with the only restriction that one dbeys eqs.(3.5d) and (3.6).

In Fig.6a-6f the six functions of eq.(3.3) are plotted as a function of the momentum transfer **q**. Results are given for the G-matrix of the meson exchange potential HEA [7] at a density corresponding to $k_F=1.2fm^{-1}$ and for an average starting energy E=-74MeV. This force is denoted in the following by G^I_{NM}. The four central functions are plotted in the same units in order to compare their momentum dependence. As argued above, it is not the absolute value of the scale

which is important but the momentum dependence in a relevant momentum interval. A relevant interval means in this case a region of momentum transfer which can still be incorporated in e.g. harmonic oscillator or Woods-Saxon wave functions relevant for ^{16}O. Such an interval will be roughly $0\text{-}3fm^{-1}$ [14],[23]. For this reason we do not attempt to fit the very high momentum components of the G-matrix. This is not difficult but the additional information is not needed in structure calculations of finite nuclei, since it is suppressed by the single-particle wave functions. Important here is only that the short-range correlations are taken care of to generate the effective G-operator.

The relevant length discussed above corresponds roughly to twice the Fermi momentum of nuclear matter at normal density ($k_F=1.36fm^{-1}$). In this unit the functions f, f',g... are plotted. Clearly all central functions show a momentum dependence , i.e. they do not correspond to δ-functions in configuration space. For the $\sigma_1\cdot\sigma_2\ \tau_1\cdot\tau_2$ this is of course not surprising since the pion contributes a long range component to g'(q). Part of this effect is however masked by the central contribution from the transverse isovector channel which is much shorter ranged (essentially this corresponds to the ρ-meson). A strong momentum transfer dependence of the interaction is also present in the scalar, isoscalar channel. This component represents the medium range attraction of the NN force and provides the binding of nuclear systems. The tensor component h is clearly very small whereas the isovector tensor force is dominated by π- an ρ-exchange as present in the bare HEA potential [24].

Clearly for the local interaction of the kind given in eq.(3.3) one can calculate in a simple way its matrix elements in e.q. a harmonic oscillator basis. We have used and extended the method of [23] where only pion-like interactions (a contribution of g' and h') are considered, to treat all direct and exchange matrix elements of eq.(3.3). Detailes are given in Chapter 2.2 and Appendix A. As in [9] we used a parametrisation of the interaction in terms of Yukawa forces. In such a picture one can speak of effective meson exchange and indeed in [8] it has been shown that for the correlation part $\tilde{G}$ ($G=V+\tilde{G}$) one effectively exchanges "mesons" with masses of 800MeV or more, confirming the short-range nature of G. One should note however, that it is arbitrary which parametrisation for the functions f, f'... one uses as long as it fits the functions displayed in Fig.6. It should be kept in mind that we try to establish a connection between a local nuclear matter G-matrix and a full ^{16}O G matrix. We are not directly fitting a local interaction to oscillator matrix elements of G-matrix as in [25]

The solution of Bethe-Goldstone equation for ^{16}O has been obtained using a method similar to the one given in [26]. A reference G-matrix is constructed using the Eden-Emery Pauli operator Q_{EE} [27] which is diagonal in c.m. representation. This reference G-matrix G_{EE} is then corrected using an oscillator Pauli operator Q_{HO} defined in terms of harmonic oscillator wave functions.

$$Q_{HO}\,|ab\rangle = \begin{cases} 0 & \text{for a or b = 0s1/2, 0p3/2 or 0p1/2 ,} \\ |ab\rangle & \text{otherwise .} \end{cases} \tag{3.7}$$

Then the oscillator G-matrix is

$$G(E) = G_{EE}(E) \tag{3.8}$$

$$+ G_{EE}(E)\ (Q_{HO}\ \frac{1}{E-Q_{HO}H_oQ_{HO}}\ Q_{HO} - Q_{EE}\ \frac{1}{E-Q_{EE}H_oQ_{EE}}\ Q_{EE})\ G(E)\ .$$

This equation is solved using matrix inversion technics including single-particle states up to $2n+l=9$ ($n=0,1,2,\ldots$). An average two hole starting energy for ^{16}O was used of -40MeV.

Since we want to test the reliability of the approximation given by the parametrisation of eq.(3.3), we will need a method to compare this interaction with the G-matrix for ^{16}O. We have therefore performed RPA calculations for the excitation spectrum of ^{16}O for both interacions, the effective meson exchange local force obtained via nuclear matter and the G-matrix calculated directly for ^{16}O. The results are summarized in Tables 5-8. Each Table refers to certain types of states according to parity (natural, unnatural) and isospin T(=0,1). The calculation is performed in a harmonic oscillator model space (b=1.72fm) including the pf-shell and the single-particle energies where taken from the neighbouring odd nuclei.

In Table 5 the results for natural parity T=0 states are given. This includes states with angular momentum and parity 0^+, 2^+, 4^+, 1^- and 3^-. The first column contains unperturbed energies, since only by comparing energy shifts for both interactions relative to the unperturbed energies one may draw useful conclusions. The second column contains the results

for the ^{16}O G-matrix. In column three the results are given for the nuclear matter effective force G^{I}_{NM} derived for a Fermi momentum $k_F=1.2fm^{-1}$ with average starting energy and c.m. momentum as choosen in [8]. Certainly there is quantitative agreement between both calculations and even a qualitative agreement except for the lowest excited states which lie higher for the nuclear matter interaction. This implies that this interraction is less attractive than the ^{16}O G-matrix. This can be understood as a consequence of the difference in starting energy for both interactions. Since ^{16}O G-matrix has a less negative starting energy than the nuclear matter interaction it is more attractive. In channels, for which the residual interaction is strongly attractive, already small modifications of the interactions yield a drastic change of the energy calculated for the lowest state. This is most clearly demonstrated by the 0^+, T=0 state. While the lowest unperturbed state lies at 27.4MeV the ^{16}O G-matrix brings this state down to 12.27MeV while with the less attractive interaction G^{I}_{NM} this state ends up at 15.38MeV.

To check the considerations about the starting energy we performed also a calculation for a nuclear matter interaction derived for $k_F=1.06fm^{-1}$ corresponding to the average density in ^{16}O and a starting energy E=-20MeV. It should be mentioned here that the additional change of Fermi momentum from $k_F=1.2fm^{-1}$ to $1.06fm^{-1}$ alone has a similar tendence to make the attraction larger. This is due to the additional phase space which becomes available for the intermediate states in the Bethe-goldstone equation. This effect however, is rather small since the dominant contribution to the cor-

relation part G comes from high-lying intermediate states. The results for this second interaction which is denoted by G^{II}_{NM} provides direct evidence for the importance of choosing the relevant starting energy in approximating the ^{16}O G-matrix. The results shown in the Tables even suggest that one should change the starting energy to get closest agreement. One can then consider the Fermi momentum k_F as a measure for the phase space which is excluded by the ^{16}O Fermi-sea. It doesn't seem to us therefore very reasonable to consider more than just this 'global' density approximation. Clearly this interaction is more attractive and on the basis of the chosen starting energy should be more attractive than the ^{16}O G-matrix. That this is indeed the case, one can infer from column four in Table 5.

Turning now to Table 6 which displays the results for the isovector natural parity states, one can observe a very good quantitative agreement between both nuclear matter interactions and the ^{16}O G-matrix. This shows that the energy dependence of the G-matrix for isovector ph-states is much less pronounced than for isoscalar states. In addition one observes the general tendency that the states are pushed up in energy due to the repulsive nature of the interaction in this channel. The very strong giant dipole state is very collective and is therefore somewhat more sensitive to the energy dependence. It corresponds to the fourth 1^- state in Table 6.

Table 7 contains the results for the isoscalar unnatural parity excitations. One observes a weak energy dependence and excellent agreement between the nuclear matter interactions and the ^{16}O G-matrix. Finally in Table 8 the results

for isovector unnatural parity (pionic) states are collected. Once again one can observe the excellent quality of the approximation of the ^{16}O G-matrix by the simple local effective forces obtained via nuclear matter.

Finally we show in Fig.7 a comparision of results of the theoretical calculation using the local effective force G^{I}_{NM} with experiment [28] for isovector states. One can see that very nice agreement is obtained implying that especially for the isovector ph-states one has obtained a trustworthy representation of a realistic G-matrix but at the same time an already realistic desription of pionic states. This makes further studies including a more realistic single-particle basis and effects of virtual isobar-hole components very interesting. Calculation of this type will be reported in Chapter 4. The isoscalar states are sometimes reasonably close to experiment. However, the 0^+, T=0 state is much to low in energy. This might be corrected if screening effects which play such an important role for infinite systems [29-32] are taken into account, or by explicit consideration of two-particle two-hole configurations.

The results discussed in this Chapter clearly show that the complicated non-local G-matrix interaction calculated for finite nuclei can very well be approximated by simple local interaction obtained from the nuclear matter in global density approximation. The comparision with experimental data indicates that the G-matrix is already a very good aproximation for the effective interaction to be used in RPA calculations of isovector states. An small additional renormalization of the residual interaction seems to be needed for isoscalar states of natural parity or explicit two-par-

ticle two-hole configuration should de considered. The success of the simple interactions encourages its application in RPA calculations of heavier systems or for other nuclear structure investigations [33].

4. SPIN-ISOSPIN EXCITATIONS COMPARISION BETWEEN FINITE NUCLEI AND NUCLEAR MATTER.

Spin-isospin excitations in nuclei have received much attention in recent years. The special interest in these states is mainly motivated by the hope that an analysis of these excitations should yield information on the exchange of pions in the nuclear medium and on the possibility of exciting nucleons which are embedded in a nucleus, to the $\Delta(3,3)$ resonance. Therefore the spin-isospin excitations may provide a direct way of studying the influence of mesonic and isobar degrees of freedom on the structure of nuclei. It has been suggested that virtual Δ-hole components in the nuclear wave function might be responsible for the experimentally observed quenching of Gamow-Teller strength [34] and magnetic transitions [35]. However, before one can answer the question to which extend non-nucleonic degrees of freedom might be needed to explain these experimental data, one has to perform reliable nuclear structure calculations of these states within the conventional framework. An important ingredient for such nuclear structure calculations of e.g. RPA kind is the residual nucleon-nucleon interaction. The effective particle-hole (ph) interaction which is now most frequently beeing use for theoretical calculations of spin-isospin excitations has the form

$$V^{ph}_{\sigma\tau}(\mathbf{q}) = V^{\pi}(\mathbf{q}) + V^{\rho}(\mathbf{q}) + \text{Phenomenology} \qquad (4.1)$$

$$= \Big[- \frac{f_\pi^2}{m_\pi^2} \frac{q^2}{m_\pi^2+q^2} \sigma_1\cdot q \sigma_2\cdot q - \frac{f_\rho^2}{m_\rho^2} \frac{q^2}{m_\rho^2+q^2} \sigma_1 x q \sigma_2 x q + g' \sigma_1\cdot\sigma_2 \Big] \tau_1\cdot\tau_2$$

This can be considered as an extension of the simple Landau-Migdal interaction, which contains just the term with the constant g' [36],[37]. One hopes that the dominant effects due to the finite range of the residual interaction in this ph channel are taken into account by the explicit consideration of π - and ρ-exchange, so that the remaining contributions arising from correlation effects and exchange terms can be described by the constant g' [38]. Different groups consider either the direct matrix elements of the finite range terms in eq.(4.1) only [39],[40], or both the direct and the exchange contribution [14],[23],[41]. Now the question is whether g' is a parameter of global meaning or just a fitting parameter which has to be readjusted depending on the system under consideration. It is the purpose of this letter to investigate this question.

In a first step we will try to find a parametrisation of the form displayed in eq.(4.1) for the ph interaction in nuclear matter. As an example for a realistic ph interaction which is determined microscopically, the Brueckner G-matrix determined by solving the Bethe-Goldstone equation for the meson exchange potential of [7], is considered. Now one may argue that a G-matrix is only a first approximation to the effective ph interaction, which shall be parametrized by eq.(4.1). If, however, it can be shown, that the ansatz of eq.(4.1) is not sufficient to represent a G-matrix one should not hope that this ansatz can describe a more complicated ph interaction. However, already the solution of the Bethe-Goldstone equation in nuclear matter is a rather complicate object. If one determines from such a G-matrix the irreducible ph interaction for ph excitations of a give spin

and isospin α, this interaction G_α still depends on three momentum variables [9]. The additional dependence of G_α on the starting energy can be treated by applying the averaging procedure discussed in [9]. Since one cannot hope that the complete momentum dependence of G_α can be obtained by adjusting g' in the parametrisation of eq.(4.1), we try to determine an optimal value of g' by requesting that the parametrisation of eq.(4.1) yields the same response function as obtained for G_α. Here it should be understood that in the full calculation direct and exchange matrix elements for the G-matrix are taken into account, for the analysis in terms of eq.(4.1) only direct matrix elements of the operator in eq.(4.1) are considered. The static response function for spin isospin excitations α of nuclear matter $\Pi_\alpha(q)$, depending on the momentum transfer q can be calculated as

$$\Pi_\alpha(q) = \Pi_\alpha^0(\mathbf{q}) + 4\int\frac{d^3p}{(2\pi)^3}\int\frac{d^3p'}{(2\pi)^3}\, g_{ph}(\mathbf{p},\mathbf{q})R_\alpha(\mathbf{p},\mathbf{p}';\mathbf{q})g_{ph}(\mathbf{p}',\mathbf{q}) \tag{4.2}$$

In this equation Π_α^0 stands for the free response function which is equal to 4 times the Lindhard function. The functions $g_{ph}(p,q)$ represent the static ph propagator depending on the total momentum $\mathbf{q}$ and the relative momentum $\mathbf{p}$ of the ph state. The reducible ph interaction R_α can be calculated from the irreducible interaction G_α by solving an integral equation, which corresponds to an inclusion of RPA correlations [30]

$$R_\alpha(p,p';q) = G_\alpha(p,p';q) + \int \frac{d^3k}{(2\pi)^3} G_\alpha(p,k;q) g_{ph}(k,q) R_\alpha(k,p';q) \tag{4.3}$$

Since in nuclear matter the spin longitudinal (pion) channel and spin transverse (ρ-meson) channel are orthogonal eqs (4.2) and (4.3) can be calculated separately for each channel α. Numerical details can be found in [9],[30]. If one now considers an irreducible ph interaction G_α which only depends on the momentum transfer k and not on the relative ph momenta, eqs (4.2) and (4.3) can be solved analytically and one can rather easily determine an effective interaction $G_{eff,\alpha}(q)$ by requesting that one obtains the same result as for the complete G-matrix. The effective $G_{eff,\alpha}$ can then be split into the contribution from the direct π-exchange (or ρ-exchange, depending on α) and function $g'_\alpha(q)$. The resulting constants g' are optimal value for the parametrisation of eq.(4.1) in order to reproduce the response function of nuclear matter for a given channel and momentum **q**. Strictly speaking one should allow for a tensor term $h'(q)\, S_{12}(\hat{q})\, \tau_1 \cdot \tau_2$ in eq.(4.1) to allow a spliting in both channels after subtraction of direct π- and ρ-exchange terms.

Results of such an anlysis for nuclear matter at normal density (k_F=1.4fm^{-1}) are displayed in Fig.8. It can be seen that the resulting g' vary only slightly with momentum transfer q and are very similar for the 2 different channels. This implies that tensor term h'(**q**) beside π- and ρ-exchange in eq.(4.1) can be neglected in this analysis of average nuclear matter quantities. An averaged numerical value for g' can be given as 0.45 in pionic units $(f_\pi/m_\pi)^2$. The weak dependence of the effective constants g' on **q** and α

gives rise to the hope that eq.(4.1) represents a usefull parametrisation of the G-matrix and g' is a constant of some global meaning.

To investigate this point a little bit more in detail, we investigate in the next step if the same parametrisation of eq.(4.1) can be used to evaluate the G-matrix elements which are relevant for an RPA calculation of the low-lying isovector states of unnatural parity in ^{16}O. Here we mention that it has recently been shown [30] that an appropriate operator representation of the solution of the Bethe-Goldstone equation in nuclear matter yields matrix elements for finite nuclei, which are in excellent agreement with those obtained for the corresponding G-matrix calculated directly for the finite nucleus. This means that the treatment of short range correlations as they are taken into account in the G-matrix is very similar for infite nuclear matter and finite nuclei. Therefore we will use for the comparison the G-matrix denoted by G^{II}_{NM} in Chapter 3, which has been determined for the same meson exchange potential HEA of [7] discussed above. In Table 9 we have listed the most important diagonal ph matrix elements which are needed for an RPA calculation of isovector states in ^{16}O. The matrix elements of G^{II}_{NM} are evaluated in a basis of oscillator single-particle wave functions, for which the oscillator constant (b=1.639 fm) has been chosen to obtain an optimal overlap with relevant Woods-Saxon wave functions. To analyse these matrix elements we also display the contributions originating from the direct and exchange terms of the bare one-π-exchange and one-ρ-exchange of the potential HEA. Looking first to the bare one-π-exchange terms one notices that the

direct terms are of course all attractive (see also Fig.8). For the diagonal matrix elements listed in this Table the exchange terms are consistently repulsive. However, it should be noticed that one finds large deviations from the rule that the exchange term is about -0.25 times the direct term, which is strictly valid for central forces of zero range only. The contribution from one-ρ-exchange is considerably weaker. Although the sum of the bare π- and ρ- terms is attractive, the matrix elements of G^{II}_{NM} are all repulsive. This is in contrast to the nuclear matter calculation (see Fig.8), where the same G-matrix turned out to be attractive in the pion channel at larger momentum transfer. This implicates that the collective behaviour evaluated in nuclear matter for the pion channel at large momentum transfer may not be observed in finite systems and therefore a typical result for nuclear matter only. This example shows that one has to be very careful in deducing long-range ph correlations in finite nuclei from those of nuclear matter.

In Table 9 we also list for the individual matrix elements those values of g', which are needed so that the parametrisation of eq.(4.1) yields the same values as G^{II}_{NM}. The values of g' displayed in the last column of Table 9 are obtained assuming that direct and exchange term of V^{π} and V^{ρ} in eq.(4.1) are taken into account, while the column next to the last is obtained if only the direct terms are considered. All the values of g' are given in pionic units and therefore the results listed in the column next to the last are directly comarable to the 0.45 obtained from the analysis in nuclear matter. The constants which are needed to represent the G-matrix in finite nuclei are considerably larger than

the values which are needed to represent the average features of the same G-matrix in nuclear matter. This and also the fact that the values of g' depend significantly on the matrix element under consideration shows clearly that the ansatz of eq.(4.1) cannot be used to evaluate individual matrix elements of G. The same is also true when exchange terms of V^{π} and V^{ρ} are trated explicitly (see last column of Table 9).

Now one may still hope that eq.(4.1) can be applied to reproduce the global features of G^{II}_{NM} which show up in the results of RPA calculations. To check this possibility we perform RPA calculations for 2^- T=1 states of ^{16}O in a small model space of 1 $\hbar\omega$ excitations. As a reference the first 2 columns of Table 10 show the results for the excitation energies and the B(M2) values as obtained by using G^{II}_{NM} for the residual interaction. The other results are obtained by using for the residual interaction the ansatz of eq.(4.1) (keeping direct or direct plus exchange terms of V^{π} and V^{ρ}) and adjusting g' in order to reproduce the excitation energy of the lowest state. The resulting values of g' (1.08 or 0.85) are again considerably larger than the 0.45 obtained in nuclear matter. But even after this adjustement of g' discrepancies in the excitation energies can be found which are as large as 1.8 MeV. Also the B(M2) values differ considerably from those obtained for G^{II}_{NM}. This demonstrates quite clearly that the ansatz of eq.(4.1) is not sufficient to represent the G-matrix. An explicit treatment of the exchange terms of V^{π} and V^{ρ} yields a slight improvement only.

An explanation for this discrepancy can only be found in the complicated momentum dependence or finite range structure of

the G-matrix. In order to understend both the differences of the G-matrix for nuclear matter and ^{16}O as well as the impossibility to represent G in terms of eq.(4.1), it is useful to consider the additional momentum dependance of G(p,p';q) beside its dependence on q. The most important variable beside q is the combination p-p', which can be thought of as a momentum carried by a meson in the exchange term. The dependence of G on the third variable p+p' is rather weak, since this momentum corresponns to the c.m. momentum in the particle-particle representation. Taking a value of p+p' as obtained by averaging over the Fermi sea, we display the G-matrix in the pion channel for a fixed value of q ($q=1.4fm^{-1}$). Note that q is chosen to be parallel to the z-axis. The remaining dependence on p-p' can be represented by $|p-p'|$ and the cosine of the angle θ between q and p-p'. In the upper part of Figure 9 we show the full G-matrix as a function of these 2 variables. Clearly there is a strong dependence of the interaction on these variables. This is due to the momentum dependence of the exchange terms, since the direct momentum q is fixed. If one subtract the middle part of Figure 9 is obtained. In this plot the dependence on $\cos\theta$ has vanished indicating that the tensor terms of the bare π- andρ-exchange are responsible for this dependence since central terms do not give a dependence on $\cos\theta$. One still observes a strong dependence on p. It is this dependence which makes the ansatz of eq.(4.1) insufficient. The reason for this additional momentum dependence can be found in the medium range of the strong scalar isoscalar correlations in G. If now in addition one subtracts the contribution from the isoscalar operators in the opera-

tor expansion of G_{NM}^{II} (effective σ-exchange, see [8]), the lower part of Fig.9 is obtained showing quite a flat function. Therefore we conclude that in addition to eq.(4.1) one has also to consider at least the finite range effects due to scalar isoscalar correlations before one can get a reliable parametrisation of G.

The exchange contribution of this part of the force is more repulsive for small values of $|p-p'|$ than for larger value of this variable (see Chapter 3). Now in nuclear matter one averages over small and large value of $|p-p'|$ (see eq.(4.3)), where as in finite nucleai like ^{16}O small values of $|p+p'|$ are dominant. This explains the more repulsive values of g' evaluated for finite nucleai as compared to the effective g' of nuclear matter evaluated for the same NN interaction.

Finally we want to demonstrate that the G-matrix alone yields an effective ph interaction which yields results for the isovector states of unnatural parity, which are in good agreement with the experimental data. For that purpose we performed RPA calculations for ^{16}O in a realistic model space. As a single-particle basis we choose the solution of a Woods-Saxon potential which was adjusted to fit the experimental single-particle states in the neighbouring odd nuclei. Continuum states are discretized and, inside an appropriate volume, expanded into harmonic oscillator wave functions [42]. Results for the isovector states are displayed in Table 11 and compared to experimental data [43],[44]. Keeping in mind that the residual interaction has been evaluated without adjusting any parameter, the agreement with experimental data is very good. It is of similar quality as

the more phenomenological calculations of [14]. Also the distribution of B(M2) strength calculated with bare magnetic operators for the nucleons is in reasonable agreement wit the data. In agreement with the results of [14] we do not get the splitting of strength around 20 MeV which is observed in experiment. More complicated components in the wave function like 3p-3h might be needed to explain this feature [45].

Concluding this chapter we would like to emphasize three points. First, it has been demonstrated that a realistic ph interaction to be used for the calculation of spin isospin excitations of nuclei cannot very well be represented by a simple π- plus ρ-exchange plus a repulsive constant g'. Already the G-matrix approximation shows a more complicated finite range structure. Secondly it should be noticed that already the G-matrix seems to be a rather good approximation to the residual ph interaction for isovector states of unnatural parity. Finally we recall that long range correlation due to collective ph excitations might be quite different in nuclear matter as compared to finite nuclei.

5. INFLUENCE OF THE Δ-ISOBARS ON THE NUCLEAR STRUCTURE AND MAGNETIC TRANSITIONS IN LIGHT NUCLEI ^{12}C AND ^{16}O.

5.1 INTRODUCTION

The interesting question in connection with spin-isospin modes in nuclei is whether subnuclear degrees of freedom might play a significant role in the low energy nuclear excitation spectra. Appart of meson degrees of freedom, the first candidate for such sonsiderations is the Δ(1232)-isobar. The Δ-isobar is reached from the nucleon by a strong ΔS=1, ΔT=1 transition. On the quark level this transition proceeds via a spin-isospin flip without changing the orbital $(1s_{1/2})^3$ quark configuration. The 300MeV mass difference between the N(938) and Δ(1232) is related to the chromomagnetic fine structure splitting. The Δ-resonance plays a dominant role in intermediate energy physics. One hopes to explain, with the help of explicit inclusion of the Δ in structure calculations, the experimentally observed quenching of Gamow-Teller and the magnetic transition strengths.

In this chapter we discuss microscopic calculations of pionlike states in ^{12}C and ^{16}O allowing for the isobar degrees of freedom. In addition other states are discussed which leads to a better understanding of the results obtained. We start with an short overview of the theoretical effects to explain the properties of pionic states in ligth nuclei. Appart from the observed quenching in Gamow-Teler strength and magnetic transitions, another posible signature of virtual isobars degrees of freedom might be visible in a

characteristic influence on the momentum dependence of isovector magnetic form factors.

The 1^+ state in ^{12}C at 15.1MeV (T=1) has been the first pionlike state whose high momentum transfer properties have been explored with sufficient accuracy in this respect. The long wavelength properties of the 1^+ state are described correctly by the conventional shell-model [46] which takes into account many-particle configurations within the p-shell. However, at large q the Cohen-Kurath shell model underestimates the magnetic form factor (1^+, T=1) by a factor 5 in the important region $q=1-2fm^{-1}$. Sugawa at al. [47] considered the first order core polarisation and exchange currents. They found that the core polarisation can account for a large part of the missing M1 strength at the high q, while exchange currents are negligible.

Toki and Weise [48] divided the physical model space into two parts. For the P-space they assumed the Cohen-Kurath p-shell wave function. The Q-space, than consist of all nucleon-hole states outside p-shell and of all $\Delta(1232)$-hole excitations. The Q-space polarisation is incorporated by employing the diamesic function technique [50] to obtain the renormalized M1 operator. The direct particle-hole interaction for π- and ρ-exchange with the additional phenomenological g' Landau parameter (g'=0.55 in pionic units) was used. With the assumption that g' is the same for the NN and ΔN channels good agreement could be obtained by fitting g' (0.55 in pionic units) to the experimental form factor. Note that this g' also simulates the exchange terms of π- and ρ-exchange.

In the Jülich version [49] of the magnetic form factor large space nuclear RPA calculations were performed using the schematic force given by eq.4.1. In addition the bare magnetic operator was renormalized. The agreement with experiment is not perfect e.g. the position of the minimum was not very well represented. In addition one must realize that the total strength has to be renormalized in RPA calculations to take into account the effect of many-particle many-hole configurations in the p-shell.

5.2 DISCUSSION AND RESULTS

As shown in Chapter 4 there is a drastric difference between collective spin-isospin correlations in infinite and finite systems. It is shown there that one cannot transfer information based on long-range correlations calculated for infinite systems to e.g. ^{16}O. The conclusion therefore is that from a microscopic point of view one should start for finite nuclei on the same level of approximation as in nuclear matter (G-matrix level) and then explicitly consider whether longe-range correlations to the effective interaction in finite nuclei are relevant. If the answer is yes these should then be explicitly calculated. In practice this means that we perform our microscopic calculation with inclusion of isobars with the G-matrix for the NN-interaction denoted in Chapter 3 by G^{II}_{NM}. For the transition $NN^{-1} \leftrightarrow \Delta N^{-1}$ we use the result (see also Chapter 2.2) of [9] that there are essentially no short-range modifications to the bare π- and ρ-exchange transition potentials.

For the $\Delta N^{-1} \leftrightarrow \Delta N^{-1}$ interaction which is any way less important in these considerations, short-range effects are non-negligable and a $g'_{\Delta\Delta}$ type interaction is added to the π- and ρ-exchange transition potentials. The value of this $g'_{\Delta\Delta}$ parameter is shown to be almost irrelevant in our calculation. The use of a microscopic effective interaction in the calculation of pionic states provides a new feature which has not been studied in the literature before. From the discussion in Chapter 4 we learned that calculations of low-lying energy excited states with pionic quantum numbers in ^{16}O show that the G-matrix, after subtraction of π- and ρ-exchange contributions, provides state dependent values of g'_N. In general, values of g'_N are larger than in nuclear matter. From the other side we have pointed out that such g'_N "parameters" depend strongly on the momentum carried by exchanged mesons and therefore it is not sufficient to replace simply g'_N by a universal constant without loosing physical informations specifically for higher momentum transfer (between 1 and 3 fm^{-1}). An important part of this chapter will be devoted to the study of the effective interaction in the calculation of excited states in ^{16}O. As shown by Meyer-ter-Vehn [23] and Speth et al.[14] it is possible with a schematic force to get reasonable agreement with experiment for the excitation energy of pionic states. Since we construct our force in a microscopic way we are in the position to consider all types of excited states like e.g. the low-lying collective 3^- and the giant resonances (2^+, 1^-) at the same time, without adjusting new parameters. This is a very stringent test on the effective interaction since with inclusion of exchange terms all types of meson exchan-

ges contribute to each type of state. To discuss the influence of the Δ-isobar in finite nuclei, we have performed RPA calculations for ^{12}C and ^{16}O. For the nucleonic excitations we have used the Woods-Saxon basis (see Chapter 2.3). Since there is no apriori reason to put the isobars in the same potential, we have used oscillator wave functions for the isobar states. The size of the single-particle space was obtained by testing the convergence of the results. Such tests for ^{12}C and ^{16}O are displayed in Tables 12,13. One can see that already with 5 major oscillator shells the calculated energies and transitions for the unnatural parity states are essentialy converged. For natural parity states this is not the case.

The space for Δ-isobars might be rather large to include possible polarisation effects of the Δ on the low-lying states. Good convergence of the results was obtained when including 8 major oscillator shells for the isobar states in the case of ^{12}C and 6 major shells for ^{16}O.

In Table 14 results of RPA calculations in ^{16}O for unnatural parity states (0^-, 2^-, 4^-) and isospin T=1 are summarized. Inclusion of Δ-isobars can only change results for T=1 states due to the fact that a Δh-states must have either isospin 1 or 2. Results show good agreement with the experimental data if we only concentrate on the position of the energies. Transition probabilities are in general overestimated. The influence of the isobar states is only marginally and increase or decrease transition probabilities depending on the individual states only slightly, differences not exceeding a few percent.

Results for isoscalar unnatural parity states can be found in Chapter 4, there it is pointed out that it is more difficult to get a good agreement with experiment although 1p-1h states are reasonably well reproduced.

As shown in Table 13, the convergence for the isoscalar natural parity states with respect to the size of the model space is not so good as for other types of states. The reason for this must be found in the attractive nature of the interaction in this channel leading to a coherent contribution of high-lying ph states. The results for these states as well as for isovector natural parity states are displayed in Table 15. We have not determined our single-particle basis selfconsistently from the effective interaction, since we prefer to use experimental single-particle energies. Nevertheless it is passible to get a feeling for the importance of having a realistic single-particle basis by comparing the results in a large madel space (10 major shells) for an harmonic oscillator (H.O.) and a Woods-Saxon basis. This is also done in Table 15. One must recall that the importance of having realistic wave functions has been repeatedly emphasized by Speth et al.. The results in Table 15 confirm this also in the case where a microscopic effective interaction is used. The energies of collective states are systematically deviating from the experimental energies e.g. the low-lying collective 0^- (T=0), the giant quadrupole (T=0) and the giant dipole (T=1) in the case of the H.O. basis. The Woods-Saxon results show a consistent agreement for essentialy all ph states collective and non-collective. This indicates that the effective interaction which is used here (G^{II}_{NM}) might be considered to be reasonable. On the other

hand an appropriate single-particle basis seems to be required. What is very striking is the fact that the transition strength for electric states is not very different for the different basis systems. To conclude the discussion on this table we want to point out that we overestimate the strength of the GDR and also of the GQR. The giant dipole resonance 1^-, T=1 state localized at about 22.3MeV with a strength of 2.4 e^2fm^2 which we overestimate by a factor 1.4. The same problem appeares for giant quadrupol resonance (2^+, T=0) states in the region of 20.7MeV. In this case we overestimate the strength by a factor 1.6. It seems therefore that also electric transitions are overestimated in this calculation. In this respect the fact that this is not the case for the low-lying 3^- state is not surprising since the energy is also not reproduced.

We now turn to the discussion of the results for ^{12}C. In Table 16 results for unnatural parity states, 0^-, 2^- ,4^- ,1^+ , are collected. Again one can see the minor influence of the isobar configurations. The most interesting state is the first 1^+, T=1 (15.1MeV) state. In the last few years people have tried to explain the high momentum transfer properties of the magnetic form factor of this state. As discussed in the introduction this state might show the influence of the isobar degrees of freedom in nuclei. In Fig.10 the results for this form factor are displayed by three curves. Details of the calculation of the general form of the magnetic form factor of any multipolarity are given in Appendix B. The dotted curve represents the pure $0p_{1/2}$-$0p_{3/2}$ state coupled to T=1. The dashed curve shows the result of the RPA calculation with the local G-operator (G^{II}_{NM}). Quite a good repro-

duction of the experimental data is obtained. The influence of the Δ-isobar is displayed as the solid curve. One can see a tendency of small quenching of the transition, in comparision with the nucleon case only, in the small momentum transfer region and some enhancment in the region from 1 to $3fm^{-1}$. This effect is due to the ΔN^{-1} interaction which is repulsive for small momentum and attractive for higher momentum transfer. In the long wave length limit the calculated quenching is only in the range of few percent (5%). The B(M1) value goes from 9.2 μ_N^2 for the nucleon case to 8.7 μ_N^2 with inclusion of isobares. To have a good comparision of the shape of all curves we have multiplied each of them by a constant $C=B(M1)_{Exp}/B(M1)_{Th}$, where $B(M1)_{Exp}$ = 2.78 μ_N^2 is the experimental value and $B(M1)_{Th}$ corespondes to the calculated value for each case (for the pure $0p_{1/2}$-$0p_{3/2}$ state $B(M1)_{Th}$ = 11.4 μ_N^2).

At this piont it is useful to discuss shortly the reason for the small influence on the Δ configurations. To ilustrate this we have performed calculations where artificially a coupling interaction $NN^{-1} \leftrightarrow \Delta N^{-1}$ was added of the g'_Δ type. Even for g'_Δ=0.1 much stronger renormalisations were observed indicating that this is indeed a parameter to get better agreement with quenched transition strengths found in experiment. As argued already in Chapter 4 and Chapter 2.2 there is on theoretical grounds based an insight in many-body renormalisation effects no explanation for this additional g'_Δ interaction. Since we find no strong collective effects treating carefully short-range correlations in the effective interaction, it is impossible to obtain large corrections due to "screening" terms which are however large in

nuclear matter [32]. The large effect in nuclear matter which is unrelated to finite nuclei is due to the attraction of the effective interaction in the pion channel in nuclear matter (see Chapter 4). This leads to the collective effects which lead to a strong screening mechanism and therefore strong induced interaction. It is important to note that g'_Δ can only come from screening terms almost independently on the form of the bare transition potential. This is related to the fact that exchange terms cancel any short-range contribution left for g'_Δ which are however small in finite nuclei as shown above.

Summarising, for the doubly closed shell nucleus ^{16}O we have a satisfactory description of the energies of essentially all states. Also for ^{12}C good agreement for the momentum-dependence of M1 form factor to the 1^+, T=1 state at 15.1MeV is achieved. Inclusion of isobar degrees of freedom, however shows hardly any influence for reasons discussed above.

Finally, considering the strength of spin-isospin transitions, we want to stress that in our calculations we typically overestimate this strength in the usual way. A remarkable feature however is that also electric transitions are overestimated, whereas the corresponding excitation energies are correctly reproduced by our G-matrix calculation. This new feature which we observe in our microscopic approach suggest that quenching is a more general phenomena than has been assumed up to now. An explanation for this must then be found in the single-particle strength (we have used 1) and additional 2p-2h admixture. Since we have included isobar

degrees of freedom in our calculation in a consistent way and found its influence to be small, we believe that low energy nuclear structure is not too strongly influenced by non nucleonic degrees of freedom.

6. CONCLUSIONS

To conclude we would like to summarize some important results and discuss some possible extensions and continuations of the present investigations.

The main point of this thesis is to discuss an influence of Δ-isobar excitations on the structure of finite nuclei. To perform the calculations we have started from the construction of a microscopic, local NN interaction. This local interaction derived from the nuclear matter G-matrix (in global density approximation) very well approximates the complicated non-local G-matrix interaction calculated for finite nuclei. The comparision with the experimental data shows a very good agreement specially for isovector states. We have demonstrated that this interaction, however can not be reproduced by a simple π- and ρ-exchange plus a repulsive constant g', a parametrisation which is frequently used in the literature.

Finally, turning to the problems connected with isobar degrees of freedom we introduced in addition to the local G-matrix the $NN^{-1} \longrightarrow \Delta N^{-1}$ interaction. In general, the influence of the Δ-isobar on the low-lying states of ^{12}C and ^{16}O is rather weak. Also the momentum dependence of the M1 form factor to the 1^+, T=0 state of ^{12}C does not change much after inclusion of the Δ excitations. One should note that already a calculation with a NN G-matrix gives a good agreement between the calculated form factor and experiment. We typicaly overestimate in our calculations all electric and magnetic transition strengths. We find that isobars influence only pionic states and do not reduce the strength, whe-

reas energy levels are correctly reproduced. From these facts one can deduce that the quenching of the M1 strength, which is very much discussed in the literature, can not be explained simply in terms of subnucleonic degrees of freedom.

Our calculations lead to the general conclusion that not Δ but other phenomena like 2p-2h excitations or a renormalisation of the single-particle strength of the RPA propagator are needed to explain the experimentaly observed quenching of magnetic transition probabilities.

Appendix A

CALCULATION OF THE MATRIX ELEMENTS OF THE G-OPERATOR

In this appendix the calculation of two-body interaction matrix elements is described. The structure of the interaction operator has a local character which allows to use a different method of calculation than the usual method which uses Moshinsky brackets. The wave function of the particle with spin s moving in spherically symmetric and parity-conserving potential to be used in this calculation can be written in the form

$$\langle \mathbf{r}| nljm\rangle = u_{nl}(r) \sum_{\substack{m_l \\ m_s}} \langle lm_l sm_s| jm\rangle i^l Y_{lm_l}(\hat{\mathbf{r}})|sm_s\rangle \ . \qquad \text{(A1)}$$

The total matrix element of any interaction V between particle-hole states coupled to total angular momentum J and isospin T looks like

$$\langle |[n_1 l_1 s_1 j_1,(n_2 l_2 s_2 j_2)^{-1}]^{JMTM_T}| V | |[n_3 l_3 s_3 j_3,(n_4 l_4 s_4 j_4)^{-1}]^{JMTM_T}\rangle \ . \qquad \text{(A2)}$$

For simplicity we introduce a short hand notation where 1 denotes a state with quantum numbers $(n_1 l_1 s_1 j_1)$. To calculate explicity such a matrix element as in eq.(A2) we change the coupling from $j_1+j_2 \Longrightarrow J$ to the $L_1+S_1 \Longrightarrow J$ and then decouple the matrix element to the orbital and spin and isospin parts (short hand notation is used $\hat{j}=[2j+1]^{1/2}$).

$$\langle 1,2^{-1}JMTM_T|V|3,4^{-1}JMTM_T\rangle = \qquad \text{(A3)}$$

$$\sum \hat{j}_1\hat{j}_2\hat{j}_3\hat{j}_4\hat{L}_1\hat{L}_2\hat{S}_1\hat{S}_2 \langle l_1 m_{l_1} l_2 m_{l_2}| L_1 M_{L_1}\rangle \langle l_2 m_{l_2} l_3 m_{l_3}| L_2 M_{L_2}\rangle$$

$$\begin{Bmatrix} l_1 & s_1 & j_1 \\ l_2 & s_2 & j_2 \\ L_1 & S_1 & J \end{Bmatrix} \begin{Bmatrix} l_3 & s_3 & j_3 \\ l_4 & s_4 & j_4 \\ L_2 & S_2 & J \end{Bmatrix} \langle L_1 M_{L_1} S_1 M_{S_1} | JM \rangle \langle L_2 M_{L_2} S_2 M_{S_2} | JM \rangle$$

$$\langle n_1 l_1 m_{l_1} (n_2 l_2 m_{l_2})^{-1} [s_1 t_1 (s_2 t_2)^{-1}]^{T} S_1 M_{S_1} T M_T | V$$

$$| n_3 l_3 m_{l_3} (n_4 l_4 m_{l_4})^{-1} [s_3 t_3 (s_4 t_4)^{-1}]^{T} S_2 M_{S_2} T M_T \rangle .$$

Here summation goes over L_1, L_2, S_1, S_2, M_{L_1}, M_{L_2}, M_{S_1}, M_{S_2}, m_{l_1}, m_{l_2}, m_{l_3}, m_{l_4}. As pointed out in Chapter 1, we are interested only in two kinds of interaction operators, namely the tensor and the central one. The tensor interaction can be written in the following way

$$V_t(q) = [V_s^t \times V_o^t]_o^o \cdot V_I \qquad \text{(A4)}$$

$$= [24\pi]^{1/2} \sum_{\mu} \langle 2\mu 2-\mu | 00 \rangle [\sigma_1 \times \sigma_2]_\mu^2 \, Y_{2-\mu}(\hat{q}) \, V_I \, V(q) ,$$

where V_I is the isospin operator (1 or $\tau_1 \cdot \tau_2$) and $V(q)$ represents the momentum transfer dependence (in r-space this corresponds to the radial dependence). The central force has the form

$$V_c(q) = V_s^c \, V_o^c \, V_I , \qquad \text{(A5)}$$

where V_s^c now corresponds to either 1 or $\sigma_1 \cdot \sigma_2$ and V_o^c is a function of q only. In spin space the direct ph matrix element of the operator $[\sigma_1 \times \sigma_2]_\mu^2$ is [3]

$$\langle s_1 s_2^{-1} \, S M_S | [\sigma_1 \times \sigma_2]_\mu^2 | s_3 s_4^{-1} \, S' M_{S'} \rangle = -\frac{1}{3} (-1)^{s_4 - s_3 - S' - M_{S'}}$$

$$\langle SM_S S'-M_{S'} | 2\mu \rangle \langle s_1 \| \sigma_1 \| s_2 \rangle \langle s_4 \| \sigma_2 \| s_3 \rangle \delta_{S,1} \delta_{S',1} \cdot \qquad \text{(A6)}$$

The matrix element of the scalar operator $\sigma_1 \cdot \sigma_2$ has a non zero value only for $S=S'$ and $M_S=M_{S'}$

$$\langle s_1 s_2^{-1} \; SM_S | \; \sigma_1 \cdot \sigma_2 \; | s_3 s_4^{-1} \; SM_S \rangle = \qquad \text{(A7)}$$

$$-\frac{1}{3} (-1)^{s_4+s_3} \langle s_1 \| \sigma_1 \| s_2 \rangle \langle s_4 \| \sigma_2 \| s_3 \rangle \delta_{S,1}$$

The matrix element of the unit operator 1 in the spin space is simply

$$\langle s_1 s_2^{-1} SM_S | \; 1 \; | s_3 s_4^{-1} SM_S \rangle = \qquad \text{(A8)}$$

$$- (-1)^{s_4+s_3} \delta_{s_1 s_2} \delta_{s_3 s_4} \delta_{S,0} \, [2s_1+1]^{1/2} \, [2s_4+1]^{1/2} \, .$$

The orbital potential has been given in momentum space. The matrix element of such a potential in the local approximation depends only on the momentum transfer q.

$$\langle \mathbf{p}_1 \mathbf{p}_2^{-1} | \; V_o \; | \mathbf{p}_3 \mathbf{p}_4^{-1} \rangle = \delta(\mathbf{p}_1+\mathbf{p}_4-\mathbf{p}_2-\mathbf{p}_3) \; V(q) \; \left\{ \begin{matrix} Y_{2-\mu}(\hat{q}) \\ 1 \end{matrix} \right. \qquad \text{(A9)}$$

where $q=|\mathbf{p}_1-\mathbf{p}_2|=|\mathbf{p}_3-\mathbf{p}_4|$ and the upper part ($Y_{2-\mu}(\hat{q})$) corresponds to the tensor force and 1 to the central force. The direct matrix element of the orbital part of the interaction in the basis defined by eq.(A1) is

$$\langle \; n_1 l_1 m_{l_1} (n_2 l_2 m_{l_2})^{-1} \; | \; V_o \; | \; n_3 l_3 m_{l_3} (n_4 l_4 m_{l_4})^{-1} \; \rangle =$$

$$= \sum_{\substack{l'\nu' \\ l\ \nu}} 4\pi\ F^{1234}_{\lambda\lambda'} \begin{cases} \langle \lambda'\nu' 2-\mu | \lambda\nu \rangle & \dfrac{(2\lambda'+1)5}{(2\lambda+1)4\pi}^{1/2} \langle 20\lambda'0|\lambda 0\rangle \\ \delta_{11'}\ \delta_{\nu\nu'} \end{cases}$$

$$\hat{l}_2\hat{l}_4 \langle \lambda 0 l_2 0 | l_1 0\rangle \langle \lambda' 0 l_4 0 | l_3 0\rangle \langle l_1 m_{l_1} l_2 m_{l_2} | \lambda\nu\rangle\ ZX\ V(q)$$

$$\langle l_3 m_{l_3} l_4 m_{l_4} | \lambda'\nu'\rangle \qquad \text{(A10)}$$

where $F^{1234}_{\lambda\lambda'} = \int dqq^2\ R^{12}_{\lambda}(q) R^{34}_{\lambda}(q)\ V(q)$ and $R^{12}_{\lambda}(q)$ is a radial matrix element calculated in Appendix C.,

$$ZX = (-1)^{l_1+\lambda'+l_4}\ (i)^{l_1+l_2+l_3+l_4+\lambda+\lambda'} \qquad \text{(A11)}$$

Using eqs(A3-10) we can write the direct matrix element, eq.(A2), for the scalar isoscalar interaction as $V = V(q)\boldsymbol{\sigma}_1\cdot\boldsymbol{\sigma}_2\ \boldsymbol{\tau}_1\boldsymbol{\tau}_2$ can be written

$$\langle 1,2^{-1}JMTM_T | V | 3,4^{-1}JMTM_T\rangle = \delta_{T,1}\ \frac{1}{3} \sum_L 4\pi(2L+1)\ \hat{j}_1\hat{j}_2\hat{j}_3\hat{j}_4\hat{l}_1\hat{l}_2\hat{l}_3\hat{l}_4$$

$$\begin{Bmatrix} l_1 & s_1 & j_1 \\ l_2 & s_2 & j_2 \\ L & 1 & J \end{Bmatrix} \begin{Bmatrix} l_3 & s_3 & j_3 \\ l_4 & s_4 & j_4 \\ L & 1 & J \end{Bmatrix} \begin{pmatrix} l_1 & l_2 & L \\ 0 & 0 & 0 \end{pmatrix} \begin{pmatrix} l_3 & l_4 & L \\ 0 & 0 & 0 \end{pmatrix} \qquad \text{(A12)}$$

$$F^{1234}_{LL} \langle s_1 \| \boldsymbol{\sigma}_1 \| s_2\rangle\ \langle s_4 \| \boldsymbol{\sigma}_2 \| s_3\rangle\ \langle t_1 \| \boldsymbol{\tau}_1 \| t_2\rangle\ \langle t_4 \| \boldsymbol{\tau}_2 \| t_3\rangle\ ZY\ ,$$

where ZY is a phase factor

$$ZY = (-1)^{l_3+L+l_4}\ (i)^{l_1+l_2+l_3+l_4}\ .$$

For the tensor interaction one has

$$V = V(q)\ S_{12}(\hat{q})\ \boldsymbol{\tau}_1\cdot\boldsymbol{\tau}_2 \qquad \text{(A13)}$$

$$= V(q)\left[24\pi\right]^{1/2} \sum_{\mu} \langle 2\mu 2-\mu|00\rangle \left[\sigma_1 x \sigma_2\right]^2_{\mu} \quad Y_{2-\mu}(\hat{q})\ \tau_1 \cdot \tau_2$$

and the direct matrix element

$$\langle 1,2^{-1}JMTM_T|V|3,4^{-1}JMTM_T\rangle = \delta_{T,1}\ \frac{1}{3}\ 4\pi\ \left[30\right]^{1/2}\ \hat{j}_1\hat{j}_2\hat{j}_3\hat{j}_4\hat{l}_1\hat{l}_2\hat{l}_3\hat{l}_4$$

$$\sum_{L_1 L_2} (2L_1+1)(2L_2+1) \begin{Bmatrix} l & L_2 & J \\ L_1 & l & 2 \end{Bmatrix} (-1)^J \qquad \text{(A14)}$$

$$\begin{Bmatrix} l_1 & s_1 & j_1 \\ l_2 & s_2 & j_2 \\ L & l & J \end{Bmatrix} \begin{Bmatrix} l_3 & s_3 & j_3 \\ l_4 & s_4 & j_4 \\ L & l & J \end{Bmatrix} \begin{pmatrix} l_1 & l_2 & L_1 \\ 0 & 0 & 0 \end{pmatrix} \begin{pmatrix} l_3 & l_4 & L_2 \\ 0 & 0 & 0 \end{pmatrix} \begin{pmatrix} L_1 & L_2 & 2 \\ 0 & 0 & 0 \end{pmatrix}$$

$$F^{1234}_{LL} \langle s_1\|\sigma_1\|s_2\rangle\ \langle s_4\|\sigma_2\|s_3\rangle\ \langle t_1\|\tau_1\|t_2\rangle\ \langle t_4\|\tau_2\|t_3\rangle\ ZZ\ ,$$

where ZZ

$$ZZ = (-1)^{l_3+L_2+l_4}\ (i)^{l_1+l_2+l_3+l_4+L_1+L_2}\ .$$

To obtain the exchange matrix element we use the general formula

$$\langle 1,2^{-1}JT|V|3,4^{-1}JT\rangle_{exch} = -\sum_{J'T'} \langle 1,2^{-1}J'T'|V|3,4^{-1}J'T'\rangle_{dir}$$

$$(-1)^{J+J'+j_2+j_3}\ (2J'+1) \begin{Bmatrix} j_4 & j_3 & J \\ j_1 & j_2 & J' \end{Bmatrix} \qquad \text{(A15)}$$

$$(-1)^{T+T'+t_2+t_3}\ (2T'+1) \begin{Bmatrix} t_3 & t_4 & T \\ t_1 & t_2 & T' \end{Bmatrix}$$

To perform RPA calculations we also need the backward going matrix elements which can be derived from the forward going ones by means of

$$\langle 1,2^{-1}JMTM_T,(3,4^{-1})JMTM_T|\,V|\,0\rangle = \qquad \text{(A16)}$$

$$(-1)^{J+j_4+j_3}\ (-1)^{T+t_4+t_3}\ \langle 1,2^{-1}JMTM_T|\,V|\,4,3^{-1}JMTM_T\rangle$$

where

$$|\,JM\rangle = (-1)^{J+M}\,|\,J-M\rangle\ . \qquad \text{(A17)}$$

Appendix B

SINGLE PARTICLE MATRIX ELEMENT FOR THE MAGNETIC FORM FACTOR.

The magnetic form factor obtained from the electron scattering is defined by:

$$\left| F_M(q) \right|^2 = \frac{4\pi}{Z^2} \frac{1}{2J+1} \left| \langle J_1 T_1 \| T_J^{Mag} \| J_2 T_2 \rangle \right|^2 , \qquad (B1)$$

where Z is the nuclear charge number. The magnetic transition operator is given by:

$$T_J^{Mag}(q) = - 1/c \int d^3r \; \mathbf{J}(r) \cdot \mathbf{A}(qr) , \qquad (B2)$$

where $\mathbf{A}(qr)$ is a solution of the vector Helmholtz equation [51]:

$$\Delta \mathbf{A}(qr) + q^2 \mathbf{A}(qr) = 0 . \qquad (B3)$$

The so called Hassen solution of eq.(B3) for the magnetic case is:

$$\mathbf{A}(qr) = \frac{\mathbf{L}}{\sqrt{L(L+1)}} j_L(qr) \; Y_{LM}(\hat{\mathbf{r}}) . \qquad (B4)$$

The $Y_{LM}(\hat{\mathbf{r}})$ is a spherical harmonics and $j_L(qr)$ a spherical bessel function, L is angular momentum operator $\mathbf{L}=1/i(\mathbf{r}\times\nabla)$. The current density takes the form:

$$J(r) = j^{o}(r) + c\nabla \times \mu(r) \ , \tag{B5}$$

where the first component on the l.h.s. is the orbital current, which comes from the moving charge of protons. In the single particle model in the approximation that particles are piont like and neglecting the exchange current of pions [52] the orbital current is given by

$$j^{o}(r) = eg^{l}(\mathbf{v}\,\delta(\mathbf{r} - \mathbf{r}_i) + h.c) \tag{B6}$$

and the spin part by

$$\mu(r) = \delta(\mathbf{r}-\mathbf{r}_i)\ \mu_N g^{s}\ \mathbf{s}_i \ , \tag{B7}$$

where g^{s}, g^{l} and μ_N are given in (5.8). Inserting eq.(B6) into eq.(B2) and using $\mathbf{v} = (1/m)\mathbf{p} = -(ih/m)\nabla$ we have for the orbital part:

$$T_L^{o}(q) = \frac{i}{\sqrt{L(L+1)}}\, g^{l}\ \mathrm{grad}(j_L(qr)\ Y_{LM}(\hat{\mathbf{r}}))\cdot\mathbf{L} \ ; \tag{B8}$$

since V comutes with L. For the spin part we put eq.(B7) into eq.(B5) and eq.(B2) and after some calculations we obtain

$$T_L^{s}(q) = \frac{i}{\sqrt{L(L+1)}}\, \mu_N g^{l}\ (\nabla \times \mathbf{s}_i)\cdot(\mathbf{r}\times\nabla)(j_L(qr)Y_{LM}(\hat{\mathbf{r}})) \ , \tag{B9}$$

where we used following vector relations:

$$(\nabla\times\mathbf{s})\cdot(\mathbf{r}\times\nabla) = ((\nabla\times\mathbf{s})\times\mathbf{r})\cdot\nabla = (\nabla(\mathbf{s}\cdot\mathbf{r}) - \mathbf{s}(\nabla\cdot\mathbf{r}))\cdot\nabla =$$
$$(\mathbf{s}\cdot\mathbf{r})\Delta - (\mathbf{s}\cdot\nabla)(d/dr)r \ . \tag{B10}$$

Since $(\Delta + q^2)(j_L(qr)Y_{LM}(\hat{r})) = 0$ we have

$$T_L^s(q) = \frac{-i\mu_N}{\sqrt{L(L+1)}} g^s \vec{s}\cdot\vec{r}\, q^2 (j_L(qr)Y_{LM}(\hat{r})) \qquad \text{(B11)}$$

$$+ \mathbf{s}\cdot\nabla(d/dr(rj_L(qr)Y_{LM}(\hat{r})))\vec{I}$$

and using the relation eq.D6 for the bessel function we obtain

$$T_L^s(q) = \frac{-i\mu_N}{\sqrt{L(L+1)}} g^s \vec{s}\cdot\vec{r}\, q^2 (j_L(qr)Y_{LM}(\hat{r})) \qquad \text{(B12)}$$

$$+ (L+1)\mathbf{s}\cdot\nabla(j_L(qr)Y_{LM}(\hat{r})) - q\mathbf{s}\cdot\nabla(rj_{L+1}(qr)Y_{LM}(\hat{r}))\vec{I} \ .$$

Now using the eqs(D7-D9) we can rewrite eq.(B8) and eq.(B12) or

$$T_L^o(q) = \frac{-2i\mu_N g^l}{\sqrt{L(L+1)}} q\left(\sqrt{\frac{L+1}{2L+1}}\, j_{L+1}(qr)\vec{Y}_{L+1}\times\vec{L}\vec{I}_M^L\right.$$

$$\left. + \sqrt{\frac{L}{2L+1}}\, j_{L-1}(qr)\vec{Y}_{L-1}\times\vec{L}\vec{I}_M^L\right) \qquad \text{(B13)}$$

and

$$T_L^s(q) = \frac{i\mu_N g^s}{\sqrt{L(L+1)}} q\left(L\sqrt{\frac{L+1}{2L+1}}\, j_{L+1}(qr)\vec{Y}_{L+1}\times\vec{s}\vec{I}_M^L\right.$$

$$\left. + \sqrt{\frac{L}{2L+1}}\, (L+1)\, j_{L-1}(qr)\vec{Y}_{L-1}\times\vec{s}\vec{I}_M^L\right) . \qquad \text{(B14)}$$

To calculate the single-particle matrix element of the magnetic transition form factor we use eqs(D10,D11). We work in the l+s=j coupling sheme

$$\langle n_1 l_1 j_1 \| T_L^{O}(q) \| n_2 l_2 j_2 \rangle = \tag{B15}$$

$$-2i\mu_N g^l (-1)^{l_1+l_2+j_2+1/2} \hat{l}_1 \hat{l}_2^2 \hat{j}_1 \hat{j}_2 \sqrt{\frac{l_2(l_2+1)}{4\pi}} \begin{Bmatrix} l_1 & l_2 & L \\ j_2 & j_1 & 1/2 \end{Bmatrix}$$

$$\Big[\sqrt{\frac{2L+3}{L}} \langle n_1 l_1 | j_{L+1}(qr) | n_2 l_2 \rangle \begin{pmatrix} l_1 & L+1 & l_2 \\ 0 & 0 & 0 \end{pmatrix} \begin{Bmatrix} L+1 & 1 & L \\ l_2 & l_1 & l_2 \end{Bmatrix}$$

$$- \sqrt{\frac{2L-1}{L+1}} \langle n_1 l_1 | j_{L-1}(qr) | n_2 l_2 \rangle \begin{pmatrix} l_1 & L-1 & l_2 \\ 0 & 0 & 0 \end{pmatrix} \begin{Bmatrix} L-1 & 1 & L \\ l_2 & l_1 & l_2 \end{Bmatrix} \Big]$$

and for the spin part

$$\langle n_1 l_1 j_1 \| T_L^{s}(q) \| n_2 l_2 j_2 \rangle = \tag{B16}$$

$$\frac{i\mu_N g^s}{\sqrt{4\pi}} (-1)^{l_1} \langle s_1 \| s \| s_2 \rangle \hat{l}_1 \hat{l}_2 \hat{j}_1 \hat{j}_2$$

$$\Big(\Big[L(2L+3) \Big]^{1/2} \langle n_1 l_1 | j_{L+1}(qr) | n_2 l_2 \rangle \begin{pmatrix} l_1 & L+1 & l_2 \\ 0 & 0 & 0 \end{pmatrix} \begin{Bmatrix} l_1 & s_1 & j_1 \\ l_2 & s_2 & j_2 \\ L+1 & 1 & L \end{Bmatrix}$$

$$- \Big[(L+1)(2L-3) \Big]^{1/2} \langle n_1 l_1 | j_{L-1}(qr) | n_2 l_2 \rangle \begin{Bmatrix} l_1 & s_1 & j_1 \\ l_2 & s_2 & j_2 \\ L-1 & 1 & L \end{Bmatrix} \begin{pmatrix} l_1 & L-1 & l_2 \\ 0 & 0 & 0 \end{pmatrix} \Big).$$

The sum of eq.(B15) and eq.(B16) gives a total magnetic form factor for nucleons e.g. for spin 1/2 particles. For $N\Delta\gamma$ interaction we calculate the reduced matrix element of operator (5.2) not in the long wave length limit e.g. we have to exchange r^L to the spherical bessel function $j_L(qr)$ in

(5.4). Reduced matrix element of such operator looks similar to eq.(B16)

$$\langle n_1 l_1 j_1 \| T_L^{s}(q) \| n_2 l_2 j_2 \rangle = \qquad \text{(B17)}$$

$$\frac{i\mu_N G_1}{\sqrt{4\pi}} \frac{m}{M} (-1)^{l_1} \langle s_1 \| S \| s_2 \rangle \hat{l}_1 \hat{l}_2 \hat{j}_1 \hat{j}_2 \langle t_1 m_{t_1} | T_3 | t_2 m_{t_2} \rangle$$

$$\left(\sqrt{L(2L+3)} \right]^{1/2} \langle n_1 l_1 | j_{L+1}(qr) | n_2 l_2 \rangle \begin{pmatrix} l_1 & L+1 & l_2 \\ 0 & 0 & 0 \end{pmatrix} \begin{Bmatrix} l_1 & s_1 & j_1 \\ l_2 & s_2 & j_2 \\ L+1 & 1 & L \end{Bmatrix}$$

$$- \left[(L+1)(2L-3) \right]^{1/2} \langle n_1 l_1 | j_{L-1}(qr) | n_2 l_2 \rangle \begin{Bmatrix} l_1 & s_1 & j_1 \\ l_2 & s_2 & j_2 \\ L-1 & 1 & L \end{Bmatrix} \begin{pmatrix} l_1 & L-1 & l_2 \\ 0 & 0 & 0 \end{pmatrix} \Big),$$

where **S** and **T** are defined in Chapter 2 eq.(2.5).

Appendix C

CALCULATION OF THE RADIAL MATRIX ELEMENT.

In this appendix we calculate the radial matrtx element of the Bessel function between harmonic oscillator states. The radial matrix element $\langle n_1 l_1 | j_L(kr) | n_2 l_2 \rangle$ can be written in other form

$$R^L_{12}(k) = \int dr r^2 \, u_1(r) j_L(kr) u_2(r) \, , \tag{C1}$$

where 1 is a short notation of two quantum numbers n_1 and l_1. The harmonic oscillator radial wave function is defined as

$$u_{nl}(r) = N \, r^l \exp[-a^2 r^2/2] \, L_n^{l+1/2}(a^2 r^2) \, , \tag{C2}$$

where a is the harmonic oscillator constant in $[fm^{-1}]$, n=0,1,2,.. , and the Laguerre polynomial

$$L_n^t(x^2) = \sum_{s=0}^{n} (-1)^n \binom{n+t}{n-s} \frac{x^{2s}}{s!} \, . \tag{C3}$$

N is a normalisation constant

$$N^2 = \frac{n! \; 2 \; a^3}{\Gamma(1+n+3/2)} \, a^{2l} \tag{C4}$$

After we insert (C2) into (C1) with the help of integral formula (see [53] eq.6.631)

$$\int x^{\mu}\, e^{-a^2x^2} j_{\nu}(bx)dx =$$

$$\frac{b^{\nu}}{2^{\nu+1} a^{\nu+\mu+1}} \sqrt{\frac{\pi}{2}}\ \frac{\Gamma((\nu+\mu+1)/2)}{\Gamma(\nu+3/2)}\ M\left(\frac{\nu+\mu+1}{2}, \nu+3/2, -b^2/4a^2\right) , \quad (C5)$$

for $\nu+\mu+1>0$ and $a^2>0$, where $M(a,b,x)$ is a Confluent Hypergeometric Function we obtain

$$R^{L}{}_{12}(k) = \frac{N_1 N_2\ k^L\ \pi^{1/2}}{\Gamma(L+3/2)2^{L+2}} \sum_{p=0}^{n_1+n_2} b_p\ \Gamma(w)\ M(w, L+3/2, -k^2/4a^2) , \quad (C6)$$

where $w = \dfrac{L+l_1+l_2+2p+3}{2}$,

and

$$b_p = \frac{(-1)^p}{p!} \sum_{s=0}^{p} \binom{n_1+l_1+1/2}{n_1-s} \binom{n_2+l_2+1/2}{n_2-p+s} \binom{p}{s}$$

Summation goes only for that s which satisfy the following conditions

$$n_1-s > 0 \text{ and } n_2-p+s > 0 , \quad (C7)$$

Using relations (see [54] eq.(13.1.27) and eq.(13.6.9)) for the Confluent Hypergeometric function

$$M(a,b,x) = e^x\ M(b-a,b,-x) \quad (C8)$$

and

$$M(-n,a+1,x) = \frac{\Gamma(a)n!}{\Gamma(n+a)} L_n^{a}(x) \qquad \text{for all n integer} \quad (C9)$$

we have

$$M(w,L+3/2,q) = e^{-q}\, L_m^{L+1/2}(q)\, \frac{m!\Gamma(L+1/2)}{\Gamma(m+L+1/2)} \quad , \tag{C10}$$

where $-m=-w+L+3/2=(L-l_1-l_2+2p)/2$, m is integer if the parity is conserved. Finaly, inserting (C10) into (C6), we have after some calculations

$$R^L_{12} = N\, \frac{k^L}{a} e^{-q} \sum_{p=0}^{n_1+n_2} b_p\, \Lambda(L,M,q) m! \quad , \tag{C11}$$

where the new function $\Lambda(L,M,q)$ we define as

$$\Lambda(L,M,q) = \sum_{i=0}^{m} q^i 2^{i-m}\, \frac{(2(m+L)+1)!!}{(2(L+i)+1)!!}\, i!(m-i)! \quad , \tag{C12}$$

where the normalisation constant takes a form

$$N^2 = \frac{n_1!n_2!}{(2(n_1+l_1)+1)!!\ (2(n_2+l_2)+1)!!}\, 2^{l_1+l_2+n_1+n_2-2L} \quad . \tag{C13}$$

The final formula eq.(C13) exist only under two conditions

$$L-l_1-l_2-2p < 0 \quad , \tag{C15a}$$

$$L+l_1+l_2 = \text{even} \quad . \tag{C15b}$$

It means for all physical matrix elements.

Appendix D

In this Appendix we collect together some formulae used in this thesis. We begin with relations for the spherical bessel function:

$$\frac{d}{dr} j_L(qr) = q j_{L-1}(qr) - \frac{L+1}{r} j_L(qr) , \tag{D1}$$

$$\frac{d}{dr} j_L(qr) - \frac{L}{r} j_L(qr) = - q j_{L+1}(qr) , \tag{D2}$$

$$\frac{d}{dr} j_L(qr) - \frac{L+1}{r} j_L(qr) = q j_{L-1}(qr) , \tag{D3}$$

$$\frac{d}{dr} r j_L(qr) - L j_L(qr) = - q j_L(qr) - (2L+1) j_{L+1} , \tag{D2}$$

$$\frac{d}{dr} r j_L(qr) + (L+1) j_L(qr) = q j_L(qr) . \tag{D5}$$

Using the following notation for the tensor product

$$[\underline{T}^k x \underline{Q}^j]^J_M \equiv \sum_{qm} \langle kqjm | JM \rangle T^k_q Q^j_m$$

we can write some useful properties of the spherical harmonics

$$\underline{v}\cdot\underline{\nabla} j_L(qr) Y_{LM}(\hat{\underline{r}}) = \tag{D6}$$

$$\sqrt{\frac{L+1}{2L+1}} \sum_m \langle L+1, M+m, 1, -m | LM \rangle Y_{L+1,M+m}(\hat{\underline{r}}) v_{-m} q j_{L+1}(qr)$$

$$+\sqrt{\frac{L}{2L+1}}\sum_m \langle L-1,M+m,1,-m|LM\rangle Y_{L-1,M+m}(\hat{\mathbf{r}})v_{-m}qj_{L-1}(qr) =$$

$$=\sqrt{\frac{L+1}{2L+1}}\,qj_{L+1}(qr)|\underline{Y}_{L+1}\mathbf{x}\mathbf{v}|^L_M+\sqrt{\frac{L}{2L+1}}\,qj_{L-1}(qr)|\underline{Y}_{L-1}\mathbf{x}\mathbf{v}|^L_M\,,$$

$$\mathbf{v}\cdot\nabla rj_L(qr)Y_{LM}(\hat{\mathbf{r}})=\sqrt{\frac{L+1}{2L+1}}\,(qj_{L+1}(qr)-j_L(qr))|\underline{Y}_{L+1}\mathbf{x}\mathbf{v}|^L_M$$

$$+\sqrt{\frac{L}{2L+1}}\,(qj_{L-1}(qr)-j_L(qr))|\underline{Y}_{L-1}\mathbf{x}\mathbf{v}|^L_M\,, \tag{D7}$$

$$\mathbf{v}\cdot\mathbf{r}j_L(qr)Y_{LM}(\hat{\mathbf{r}})= \tag{D8}$$

$$j_L(qr)\left(\sqrt{\frac{L+1}{2L+1}}\,|\underline{Y}_{L+1}\mathbf{x}\mathbf{v}|^L_M+\sqrt{\frac{L}{2L+1}}\,|\underline{Y}_{L-1}\mathbf{x}\mathbf{v}|^L_M\right)\,,$$

The reduced matrix element for the tensor operator is

$$\langle n_1l_1j_1\|j_I|\underline{Y}_I\mathbf{x}\mathbf{L}|^L\|n_2l_2j_2\rangle = \tag{D9}$$

$$(-1)^{l_1+l_2+j_2+1/2}\,\langle n_1l_1|j_I(qr)|n_2l_2\rangle\,\hat{I}_2\hat{I}\hat{L}\hat{l}_1\hat{j}_1\hat{j}_2$$

$$\sqrt{\frac{l_2(l_2+1)}{4\pi}}\begin{Bmatrix} l_1 & l_2 & L\\ j_2 & j_1 & 1/2\end{Bmatrix}\begin{Bmatrix} I & 1 & L\\ l_1 & l_2 & l_1\end{Bmatrix}\begin{pmatrix} l_1 & I & l_2\\ 0 & 0 & 0\end{pmatrix}$$

$$\langle n_1l_1j_1s_1\|j_I|\underline{Y}_I\mathbf{x}\mathbf{s}|^L\|n_2l_2j_2s_2\rangle = \tag{D10}$$

$$(-1)^{l_1}\,\langle n_1l_1|j_I(qr)|n_2l_2\rangle\,\hat{I}_1\hat{I}\hat{L}\hat{I}_2\hat{j}_1\hat{j}_2\,\frac{1}{\sqrt{4\pi}}\,\langle s_1\|\mathbf{s}\|s_2\rangle$$

$$\begin{Bmatrix} l_1 & s_1 & j_1\\ l_2 & s_2 & j_2\\ I & 1 & L\end{Bmatrix}\begin{pmatrix} l_1 & I & l_1\\ 0 & 0 & 0\end{pmatrix}.$$

Refrrences

[1] T.Hamanda and I.Johnson: Nucl.Phys., **36**, (1962), 382

[2] R.Reid: Ann. of Phys., **50**, (1968), 411

[3] F.Tabakin: Ann. of Phys., **30**, (1964), 51

[4] M.M.Negels, T.A.Rijken and J.J.Swart: Phys.Rev., **D15**, (1977), 2547

[5] G.E.Brown and A.D.Jackson: "The Nucleon-Nucleon Interation", North Holland Publ. Company (Amsterdam,1976)

[6] K.Erkelenz: Phys.Rep., **13C**, (1974), 191-258

[7] K.Holinde, K.Erkelenz and R.Alzetta: Nucl.Phys., **A194**, (1972), 161

[8] W.H.Dickhoff: Nucl.Phys., **A399**, (1983), 287

[9] W.H.Dickhoff, A.Faessler, J.Meyer-ter-Vehn and H.Müther: Phys.Rev., **C23**, (1981), 1154

[10] H.Sugawara, F. von Hippel: Phys.Rev., **178**, (1968), 1764

[11] J.Speth, E.Werner and W.Wild: Phys.Rep. **23C**, (1977), 127

[12] C.Mahaux and H.A.Weidenmüller: "Shell-Model Approch to Nuclear Reactions", North Holland, Amsterdam, 1969

[13] V.Klemt: Thesis, München, (1970), unpublished

[14] J.Speth, V.Klemt, J.Wambach and G.E.Brown: Nucl.Phys., **A343**, (1980), 382

[15] H.Pilkuhn: "The Interaction of Hadrons", North Holland, Amsterdam, 1969

[16] E.Grecksch, M.Dillig and W.Knüpfer: Z.Phys, **A320**, (1981), 247

[17] Z.Blomqvist, H.Laqet: Nucl.Phys.,**A280**,(1977),450

[18] W.Pfeil, D.Schwela: Springer Tracts Modern Physics, Vol.55, p.213, Springer Verlag 1970

[19] A.Mekijan and L.Zamick: Phys.Rep., **95C**, (1983), 321

[20] J.Shurpin, T.T.S.Kuo and D.Strottman: Nucl.Phys., **A408**, (1983), 310

[21] H.A.Bethe and J.Goldstone: Proc.Roy.Soc., (London), **A238**, (1957), 551

[22] B.D.Day: Phys.Rev., **C24**, (1981), 1203

[23] J.Meyer-ter-Vehn: Phys.Rep., **74C**, (1981), 323

[24] W.H.Dickhoff, A.Faessler and H.Müther: Phys.Rev.Lett., **49**, (1982), 1902

[25] G.Bertsch, J.Borysowicz, H.McManns and W.G.Love: Nucl.Phys., **A284**, (1977), 399

[26] P.U.Sauer: Nucl.Phys., **A150**, (1970), 467

[27] R.J.Eden and V.J.Emery: Proc.Roy.Soc., (London), **A248**, (1958), 266

[28] F.Ajzenberg-Selove: Nucl.Phys., **A375**, (1982), 1

[29] S.Babu and G.E.Brown: Ann. of Phys., **78**, (1973), 1

[30] W.H.Dickhoff, A.Faessler, J.Meyer-ter-Vehn and H.Müther: Nucl.Phys., **A368**, (1981), 445

[31] W.H.Dickhoff, A.Faessler, H.Müther and S.S.Wo: Nucl.Phys., **A405**, (1983), 534

[32] H.Müther: "Nucleon-nucleon interaction and nuclear many-body problems", Eds. S.S.Wu and T.T.S.Kuo (World Scientific, Singapore, 1984);
W.H.Dickhoff: Prog. in Particle and Nuclear Physics, Ed. D.H.Wilkinson, (Pergamon, Oxford, 1984)

[33] P.W.Hengeveld, K.Allaart and W.H.Dickhoff
to be published

[34] C.D.Goodman:"Proc.Int.Conf.Nuclear Physics",Florence, eds. P.Blasi and R.A.Ricci, Vol 2, (1983), p 165

[35] A.Richter: "Proc.Int.Conf.Nuclear Physics", Florence, eds. P.Blasi and R.A.Ricci, Vol 2, (1983), p 189

[36] A.B.Migdal: "Theory of finite Fermi systems and applications to atomic nucleai", (Wiley,New York, 1967)

[37] J.Speth, E.Werner and W.Wild: Phys.Rep. **23C**, (1977), 127

[38] M.Anastasio and G.E.Brown: Nucl.Phys. **A285**, (1977), 561

[39] J.Delorme, M.Ericson, A.Figureau and N.Giraud: Phys. Lett. **89B**, (1980), 327; and **91B**, (1980), 328

[40] E.Oset,H.Toki and W.Weise: Phys.Rep. **83C**, (1982), 281

[41] J.Meyer-ter-Vehn: "Proc.Symp. on Relativistic Heavy Ion Research, GSI Report P-5, (Darmstadt,1978), 302

[42] P.Czerski, W.H.Dickhoff, A.Feassler and H.Müther: to be published

[43] F.Ajzenberg-Selove: Nucl.Phys. **A281**, (1977), 1

[44] G.Küchler, A.Richter, E.Spancer, W.Steffen and W.Knüpfer: Nucl.Phys. **A406**, (1983), 473

[45] D.J.Millener and D.Kurath: Nucl.Phys. **A255**, (1975), 315

[46] S.Cohen and D.Kurath: Nucl.Phys. **A73**, (1965), 1

[47] H.Sugawa, T.Suzuki, H.Hyuga and A.Arima: Nucl.Phys., **A322**, (1979), 361

[48] H.Toki and W.Weise: Phys.Rev.Lett. **47**, (1979), 1034

[49] T.Suzuki, F.Osterfeld and J.Speth: Phys.Lett. **100B**, (1981), 443

[50] H.Toki and W.Weise: Phys.Lett. **98B**, (1980), 265

[51] P.M.Morse and H.Feshbach: "Methods of Theoretical Physics", McGraw Hill, New York, N.Y.1953

[52] A.De Shalit and H.Feshbach: Theoretical Nuclear Physics Vol.I, Nuclear Structure, New York, 1974

[53] I.S.Gradsteyn, I.M.Ryzhik: "Tables of Integrals, Series and Products", Academic Press, N.Y.1965

[54] M.Abramowitz, I.A.Stegun: "Handbook of Mathematical Functions", Dover Publications, INC., N.Y.1972

[55] J.Flanz et al.: Phys.Rev.Lett. **43**, (1979), 1922

[56] B.T.Chertok et al.: Phys.Rev. **C8**, (1973), 23

[57] K.W.Jones et al.: Phys.Lett., **128B**, (1983), 281

Figure Captions

Fig.1: Structure of the RPA matrices. a) represents matrix A for forward-going matrix elements. b) is the B-matrix for backward-going matrix elements. By bra and ket we indicate the particle-hole states between which matrix elements are calculated.

Fig.2a: Single-particle space for ^{16}O. The levels up to the pf-shell are included.

Fig.2b: Single-particle space for ^{12}C. The levels up to the pf-shell are included.

Fig.3: Woods-Saxon wave functions for bound states of ^{16}O, parameters of the potential are given in Table 1.

Fig.4: Woods-Saxon wave functions for resonances of ^{16}O, parameters of the potential are given in Table 1.

Fig.5: Diagram a) represents the direct contribution to the particle-hole matrix element. Spin isospin quantum numbers of the ph-states put severe restrictions on the interaction operator or equivalently the type of 'effective meson' which can be exchanged. This is not the case for the exchange contribution b).

Fig.6: The six functions f, f', g, g', h and h' representing the local effective interaction $G(q;E,\rho)$ are displayed as a function of k. The bare interaction

corresponds to the HEA potential of [7]. The Fermi momentum $k_F=1.2fm^{-1}$ and the starting energy E=-74MeV have the values used in [8]. This force id denoted by G^I_{NM} The four central functions have the same scale. Noteworthy is the strong momentum dependence in the scalar isoscalar channel (f) which is even stronger than that in the pion channel (g'). The tensor component (h) is negligible whereas h' is totally dominated by the bare π- and ρ-exchange tensor force [24].

Fig.7: Excitation energies of isovector states in ^{16}O using the local effective force G^I_{NM} defined in the text. The left column corresponds to the theoretical natural parity states while the right column coresponds to unnatural parity (pionic) states. The middle column gives the experimental values taken from [28].

Fig.8: Results are displayed for an analysis of the full G-matrix in nuclear matter in terms of the parametrisation of eq.(7.1). The strength of the interaction has been determined by requiring the same results for the response function (eq.(7.2)) as obtained for the complete G. The two isovector S=1 particle-hole channels are considered for nuclear matter at normal density. In the left part of One-Pion exchange (full curve) from the avarage repulsive strength (dashed curve). A similar analysis for the ρ channel is given in the right part of the Figure. The

total average interaction for a given momentum transfer q is obtained by adding the dashed and the full curve.

Fig.9: Momentum dependence of the G-matrix in the pion-channel. For a fixed value of **q** and an average value of **p+p'**, G(**p**,**p'**;**k**) is displayed as a function of |**p**-**p'**| and the cosΘ of the angel Θ between **q** and **p**-**p'**. While the upper part shows the complete G, the middle part of the Figure is obtained after subtracting π and ρ-exchange of the bare potential. If in addition in G (see [8]) are subtracted, the lower part is obtained.

Fig.10: Results for the M1 form factor in ^{12}C. Dotted curve: pure $0p_{1/2}0\text{-}p_{3/2}$ state coupled to T=1. Dashed curve: RPA calculation with G^{II}_{NM} interaction. Solid curve: RPA calculation with Δ-isobar. Experimental data are taken from [55],[56].

TABLE 1a. Woods-Saxon potential parameters which provide a reasonable description of the single-particle spectrum of ^{12}C. V_o is the depth of the potential well (in MeV), R is the radius and the is surface width (both in fm), V_{LS}, R_{LS} and a_{LS} are the corresponding parameters of the spin orbit term. R_c is the Coulomb radius (in fm). The harmonic oscillator constant b=1.58fm.

^{12}C	V_o	R	a	V_{LS}	R_{LS}	a_{LS}	R_c
protons	-58.00	2.80	0.53	5.490	2.80	0.53	2.86
neutrons	-56.00	2.80	0.53	5.470	2.80	0.53	0.00

TABLE 1b. Woods-Saxon potential parameters for ^{16}O. The harmonic oscillator constant b=1.639fm. For further details see Table 1a.

^{16}O	V_o	R	a	V_{LS}	R_{LS}	a_{LS}	R_c
protons	-52.88	3.08	0.53	5.589	3.08	0.53	3.15
neutrons	-53.14	3.08	0.53	5.186	3.08	0.53	0.00

TABLE 2. Parameters for the description of the G^{I}_{NM} force without bare interaction, k_F=1.2fm^{-1}, E=-74MeV

Interaction symmetry	Strength	Mass [MeV]
$\sigma_1 \cdot \sigma_2 \ \tau_1 \cdot \tau_2$	1.2993	475.0
$\sigma_1 \cdot \sigma_2$	-24.294	800.0
$\tau_1 \cdot \tau_2$	34.432	725.0
$\tau_1 \cdot \tau_2$	-119.37	1500.0
1	-22.347	600.0
1	-228.74	1550.0
$S_{12}(\hat{q}) \ \tau_1 \cdot \tau_2$	-0.031	450.0
$S_{12}(\hat{q})$	51.99	1750.0

TABLE 3. Parameters for the description of the bare V interaction.

Meson	Symmetry	Strength	Mass [MeV]
π	$\sigma_1 \cdot \hat{q}\ \sigma_2 \cdot \hat{q}\ \tau_1 \cdot \tau_2$	0.9	138.5
ρ	$\sigma_1 x \hat{q}\ \sigma_2 x \hat{q}\ \tau_1 \cdot \tau_2$	-17.53	590.0
η	$\sigma_1 \cdot \hat{q}\ \sigma_2 \cdot \hat{q}$	-30.62	725.0
ς	$\sigma_1 x \hat{q}\ \sigma_2 x \hat{q}$	-42.99	810.0
1	1	-59.345	500.0
2	1	353.35	850.0
3	1	-633.71	1500.0
I1	$\tau_1 \cdot \tau_2$	22.536	700.0
I2	$\tau_1 \cdot \tau_2$	-130.07	1200.0

TABLE 4. Parameters for the description of the G_{NM}^{II} force without bare interaction, $k_F=1.06 fm^{-1}$, E=-20MeV

Interaction symmetry	Strength	Mass [MeV]
$\sigma_1 \cdot \sigma_2 \ \tau_1 \cdot \tau_2$	1.9187	450.0
$\sigma_1 \cdot \sigma_2$	-14.86	650.0
$\tau_1 \cdot \tau_2$	27.691	625.0
$\tau_1 \cdot \tau_2$	-108.43	1500.0
1	-31.245	575.0
1	-146.35	1600.0
$S_{12}(\hat{q}) \ \tau_1 \cdot \tau_2$	0.0	0.0
$S_{12}(\hat{q})$	560.0	3000.0

TABLE 5 : Comparision of nuclear matter effective interactions G^{I}_{NM} and G^{II}_{NM} and the ^{16}O G-matrix used in an RPA calculation for isoscalar natural parity states. The numbers given in parantesis represent the energy shift with respect to the unperturbed energy displayed in column 2.

J^{π}	Unperturbed Energy[MeV]	^{16}O G-matrix E=-40MeV	G^{I}_{NM} E=-74MeV k_F=1.2fm^{-1}	G^{II}_{NM} E=-20MeV k_F=1.2fm^{-1}
0^+	27.40	12.3 (-15.1)	15.4 (-12.0)	10.3 (-17.1)
	32.60	29.6 (-3.0)	31.7 (-0.9)	31.2 (-1.4)
	37.90	35.9 (-2.0)	34.7 (-3.2)	34.6 (-3.3)
2^+	26.30	19.3 (-7.0)	19.8 (-6.5)	18.0 (-8.3)
	27.20	24.2 (-3.0)	25.4 (-1.8)	25.0 (-2.2)
	31.90	31.6 (-0.3)	32.0 (+0.1)	31.9 (+0.0)
4^+	20.90	20.2 (-0.7)	19.9 (-1.0)	19.6 (-1.3)
	27.20	27.2 (+0.0)	27.0 (-0.2)	26.9 (-0.3)
1^-	12.00	9.26 (-2.74)	10.7 (-1.3)	10.1 (-1.9)
	16.60	18.4 (+1.8)	18.5 (+1.9)	18.3 (+1.7)
	17.80	20.6 (+2.8)	20.3 (+2.5)	20.1 (+2.3)
3^-	11.50	7.75 (-3.75)	8.41 (-3.09)	7.2 (-4.3)
	17.80	17.1 (-0.7)	17.1 (-0.7)	16.9 (-0.9)
	22.90	23.2 (+0.3)	23.9 (+1.0)	23.7 (+0.8)

TABLE 6 : Comparision of nuclear matter effective interactions and the ^{16}O G-matrix used in an RPA calculation for isovector natural parity states. For further details see Table 4.

J^π	Unperturbed Energy [MeV]	^{16}O G-matrix E=-40MeV	G^{I}_{NM} E=-74MeV k_F=1.2fm^{-1}	G^{II}_{NM} E=-20MeV k_F=1.2fm^{-1}
0^+	27.40	27.6 (+0.2)	27.6 (+0.2)	27.8 (+0.4)
	32.60	35.3 (+2.7)	34.9 (+2.3)	35.7 (+3.1)
	37.90	43.6 (+5.7)	42.4 (+4.5)	44.5 (+6.6)
2^+	26.30	27.2 (+0.9)	27.4 (+1.1)	27.6 (+1.3)
	27.20	29.6 (+2.4)	29.3 (+2.1)	29.7 (+2.5)
	31.90	32.6 (+0.7)	32.5 (+0.6)	32.7 (+0.8)
4^+	20.90	22.3 (+1.4)	22.2 (+1.3)	22.4 (+1.5)
	27.20	28.0 (+0.8)	27.8 (+0.6)	28.0 (+0.8)
1^-	12.00	13.1 (+1.1)	13.3 (+1.3)	13.7 (+1.7)
	16.60	17.7 (+1.1)	17.7 (+1.1)	17.9 (+1.3)
	17.80	20.5 (+2.7)	20.2 (+2.4)	20.7 (+2.9)
	18.50	23.2 (+4.7)	22.4 (+3.9)	23.8 (+5.3)
	22.90	26.1 (+1.9)	25.8 (+2.9)	26.5 (+3.6)
3^-	11.50	13.4 (+1.9)	13.3 (+1.8)	13.6 (+2.1)
	17.80	18.9 (+1.1)	18.7 (+0.9)	19.0 (+1.2)
	22.90	24.9 (+2.0)	24.9 (+2.0)	25.4 (+2.5)

TABLE 7 : Comparision of nuclear matter effective interactions and the ^{16}O G-matrix used in an RPA calculation for isoscalar unnatural parity states. For further details see Table 4.

J^π	Unperturbed Energy [MeV]	^{16}O G-matrix E=-40MeV	G^{I}_{NM} E=-74MeV k_F=1.2fm^{-1}	G^{II}_{NM} E=-20MeV k_F=1.2fm^{-1}
1^+				
	26.30	25.3 (-1.0)	25.9 (-0.4)	25.1 (-1.2)
	27.40	26.0 (-1.4)	27.1 (-0.3)	26.3 (-1.1)
3^+				
	20.90	21.7 (+0.8)	21.5 (+0.6)	21.4 (+0.5)
	27.20	26.7 (-0.5)	27.1 (-0.1)	26.9 (-0.3)
0^-				
	12.00	9.26 (-2.74)	9.28 (-2.72)	9.27 (-2.73)
	22.90	19.5 (-3.4)	19.4 (-3.5)	19.2 (-3.7)
2^-				
	11.50	11.9 (+0.4)	11.5 (+0.0)	11.3 (-0.2)
	16.60	16.1 (-0.5)	17.0 (+0.4)	16.8 (+0.2)
	17.80	17.6 (+0.2)	17.5 (+0.3)	17.4 (+0.4)
	18.50	19.9 (+1.4)	20.0 (+1.5)	19.8 (+1.3)
	22.90	23.1 (+0.2)	22.9 (+0.0)	22.7 (-0.2)
4^-				
	17.80	19.4 (+1.6)	19.5 (+1.7)	19.3 (+1.5)

TABLE 8 : Comparision of nuclear matter effective interactions and the ^{16}O G-matrix used in an RPA calculation for unnatural parity isovector states. For further details see Table 4.

J^π	Unperturbed Energy [MeV]	^{16}O G-matrix E=-40MeV	G^{I}_{NM} E=-74MeV k_F=1.2fm^{-1}	G^{II}_{NM} E=-20MeV k_F=1.2fm^{-1}
1^+				
	26.30	27.3 (+1.0)	27.2 (+0.9)	27.5 (+1.2)
	27.40	28.3 (+0.9)	28.0 (+0.6)	28.5 (+1.1)
3^+				
	20.90	22.0 (+1.1)	22.5 (+1.1)	22.2 (+1.3)
	27.20	28.1 (+0.9)	28.1 (+0.9)	28.4 (+1.2)
0^-				
	12.00	12.8 (+0.8)	12.7 (+0.7)	13.0 (+1.0)
	22.90	25.3 (+2.4)	24.9 (+2.0)	25.7 (+2.8)
2^-				
	11.50	13.5 (+2.0)	13.4 (+1.9)	13.6 (+2.1)
	16.60	16.7 (+0.1)	16.5 (-0.1)	16.9 (+0.3)
	17.80	19.0 (+1.2)	19.1 (+1.3)	19.4 (+1.6)
	18.50	20.6 (+2.1)	20.5 (+2.0)	21.0 (+2.5)
	22.90	24.4 (+1.5)	24.5 (+1.6)	24.6 (+1.7)
4^-				
	17.80	18.9 (+1.1)	18.7 (+0.9)	19.0 (+1.2)

TABLE 9. Analysis of matrix elements in terms of $V^{\pi} + V^{\rho} + g'$ for different angular momenta (0^-, 2^-, 4^-) and isospin T=1.

	V^{π}_{dir}	V^{π}_{exch}	V^{ρ}_{dir}	V^{ρ}_{exch}	G^{II}_{NM}	$G^{II}_{NM}-V_D$ g'	$G^{II}_{NM}-V_E$ g'
0^-							
$1d_{1/2},0p^{-1}_{1/2}$	-3.94	2.25	0.0	-.75	1.51	1.14	.83
$0d_{3/2},0p^{-1}_{3/2}$	-7.80	3.71	0.0	-.71	2.86	.88	.63
2^-							
$0d_{5/2},0p^{-1}_{1/2}$	-1.27	.37	-.51	.15	2.97	.78	.70
$0d_{5/2},0p^{-1}_{3/2}$	-1.80	.83	-.34	.15	2.73	.91	.72
$1s_{1/2},0p^{-1}_{3/2}$	-1.58	.31	-.88	-.13	1.58	.85	.81
$0d_{3/2},0p^{-1}_{1/2}$	-3.35	.64	-.61	.11	.81	.79	.66
$0d_{3/2},0p^{-1}_{3/2}$	-.63	.74	-.29	-.14	1.92	1.17	.92
4^-							
$0d_{5/2},0p^{-1}_{3/2}$	-2.91	.46	-1.22	.10	1.29	.69	.62

Diagonal matrix elements for different contributions to the particle-hole interaction are listed. The last 2 columns contain the result for g' if the G-matrix (G^{II}_{NM}) is decomposed into $V^{\pi} + V^{\rho} + g'$. If in this decomposition only direct matrix elements of V^{ρ} are considered the last but one column is obtained whereas the last column is obtained when also exchange terms are taken into account. The results for the matrix elements (columns 2-6) are given in MeV and the resulting values of g' (columns 7 and 8) are given in pionic units $(f_{\pi}/m_{\pi})^2$.

TABLE 10. Results for 2^-, T=1 states calculated in a small space ($1\hbar\omega$) using different interactions.

G^{II}_{NM}		$(V^{\pi}+V^{\rho})_{D+E}+g'(=0.85)$		$(V^{\pi}+V^{\rho})_{D}+g'(=1.08)$	
Ex	B(M2)	Ex	B(M2)	Ex	B(M2)
[MeV]	$[\mu_N^2 fm^2]$	[MeV]	$[\mu_N^2 fm^2]$	[MeV]	$[\mu_N^2 fm^2]$
13.62	222.2	13.62	81.4	13.62	39.6
16.46	16.4	17.98	8.9	18.27	24.3
19.33	17.9	19.66	4.1	19.85	28.8
20.72	869.6	21.77	664.8	22.59	500.0
24.53	159.6	25.03	277.6	25.72	393.4

The results for the G-matrix are listed in the first 2 columns. The next 2 columns are obtained by assuming the residual interaction to be given by $(V^{\pi} + V^{\rho})$ + g' taking direct and exchange terms and adjusting g' to get the same excitation energy for the lowest state. The last 2 columns are obtained by considering the direct terms of π- and ρ-exchange only, readjusting g'.

TABLE 11. Unnatural parity states in ^{16}O. Comparision of realistic G-matrix calculations with experiment.

	Experiment			Theory		
	E [MeV]	(T)	B(M2) [$\mu_N^2 fm^2$]	E [MeV]	(T)	B(M2) [$\mu_N^2 fm^2$]
0^-	10.96	(0)		10.46		
	12.80	(1)		12.41	(1)	
	15.10			19.63		
2^-	8.87	(0)		11.53		1.0
	12.53	(0)	38±9	13.16	(1)	235.9
	12.96	(1)	121±24	16.69		1.4
	13.98			16.70		25.1
	15.22			17.17		18.2
	16.82		19±2	18.88	(1)	18.9
	17.78		13±2	19.44		12.4
	18.50		59±7	20.57	(1)	941.0
	19.00	(1)	341±51	22.28		0.0
	20.30	(1)	461±162	23.89	(1)	110.6
	20.30		~100			
4^-	17.79	(0)		18.77		
	18.98	(1)		18.95		
	19.80	(0)		40.06		

For the 2^- state we also compare the B(M2) values observed in experiment [43],[44] with the results of the calculation. The values listed in brackets following the experimental excitation energies corresponds to the isospin, for the calculated states we indicated those states by (T=1), which have strong isovector components.

TABLE 12. Test of the convergence with respect to the number of major oscillator shells N of the RPA results with the G^{II}_{NM} interaction. The test is performed for unnatural parity states in ^{12}C. Energies and magnetic transition probabilities (in $\mu_N^2 fm^{2J-2}$ units) are displayed. A small letter k after a number means that the number should be multiplied by 1000. When the calculated states has predominantly isospin 0 or 1, the isospin is explicitely given.

	E[MeV]	B(MJ)	E[MeV]	B(MJ)	E[MeV]	B(MJ)	E[MeV]	B(MJ)
J^π,T	N=2		N=5		N=8		N=10	
0^-,0	16.47	.03	16.10	.04	16.04	.04	16.01	.04
1	22.57	.01	22.43	.02	22.36	.02	22.36	.02
1^+,0	12.67	.001	11.90	.004	11.77	.005	11.74	.005
1	16.84	9.652	16.53	9.598	16.48	9.620	16.45	9.644
2^-,0	15.5	15.	15.39	16.9	15.33	17.8	15.32	17.5
1	16.81	19.	16.5	26.2	16.43	26.3	16.4	26.4
	17.3	64.	17.07	39.7	16.88	27.0	16.8	23.4
1	18.68	574.	18.56	581.	18.5	592.	18.48	594.
0	19.97	.44	19.78	.005	19.74	.09	19.73	.13
1	21.83	118.	21.67	102.	21.64	99.4	21.63	98.6
4^-	17.42	346k	17.36	292k	17.28	232k	17.23	206k
	17.65	108k	17.55	143k	17.44	199k	17.38	225k

TABLE 13. Test of the convergence of the RPA results for ^{16}O with respect to the number of oscillator shells N. Magnetic transitions are given in $\mu_N^2 fm^{2J-2}$ electric transitions are given in units $e^2 fm^{2J}$. For 2^+ states in the first column we display results for N=3 instead of N=2. For further details see Table 12. Table 13 is on the next page.

TABLE 14. Results for unnatural parity states of ^{16}O of oredominantly isovector nature are summarized. In the first column we have nucleon-nucleon results of RPA calculations with the G^{II}_{NM} interaction in the single-particle space of 5 major oscillator shells. In the second column results with inclusion of the Δ-isobar are displayed. 6 major oscillator shells of Δ states are included. The last column shows experimental data.

J^π	E[MeV]	B(MJ)	E[MeV]	B(MJ)	E[MeV]	B(MJ)
	nucleon-nucleon		delta-nucleon		Experiment	
0^-						
	12.58		12.28		12.8	
2^-						
	13.2	236.	13.15	228.	12.96	121±24
	16.9	6.9	16.5	6.8	16.82	19±24
	18.94	22.6	18.87	19.9	18.5	59±7
	20.54	941.	20.48	954.	19.	341±51
	23.98	115.	23.88	107.	20.36	465±160
4^-						
	18.88		18.87		18.98	

J^{π},T	E[MeV]	B(MJ)	E[MeV]	B(MJ)	E[MeV]	B(MJ)	E[MeV]	B(MJ)
	N=2		N=5		N=8		N=10	
0^-,0	11.41		10.84		10.46		10.29	
1	12.77		12.58		12.41		12.27	
0	20.05		19.75		19.63		19.59	
1^-,0	11.66		11.07		10.86		10.84	
1	13.65		13.52		13.47		13.46	
1	17.68		17.51		17.4		17.39	
0	17.83		17.64		17.59		17.58	
0	19.36		19.15		19.1		19.1	
1	20.21		20.06		20.0		20.0	
1	23.04	3.5	22.65	3.27	22.6	3.23	22.6	3.2
1	25.36	.65	24.93	.61	24.9	.61	24.9	.61
2^-,0	11.85	1.5	11.66	1.2	11.53	.99	11.52	1.01
1	13.32	235.	13.2	236.	13.16	237.	13.15	236.
0	16.9	20.6	16.77	21.8	16.7	25.1	16.68	23.4
1	17.03	9.6	16.9	6.9	16.68	1.4	16.63	2.7
0	17.45	16.9	17.31	16.9	17.17	18.2	17.16	18.3
1	19.03	24.4	19.6	22.6	19.4	12.4	19.4	13.3
0	20,65	951.	20.54	941.	20.5	941.	20.5	942.
2^+,0	23.8	71.	21.76	80.7	21.31	78.8	21.26	78.6
0	26.07	.3	25.77	3.35	25.65	4.7	25.63	5.01
3^-,0	8.61	654.	7.53	1010	6.94	1260	6.89	1273
1	13.53	160.	13.36	152.	13.28	153.	13.28	153.
4^-,1	18.97	388k	18.88	288k	18.77	178k	18.69	129k
0	19.21	209k	19.07	265k	18.95	369k	18.9	419k

TABLE 15. Results for natural parity states of ^{16}O are summarized. We shoe results for harmonic oscillator and Woods-Saxon wave functions in both calculations 10 major shells were taken into account. For the Woods-Saxon calculation the experimental energies are remarkably well reproduced for a parameter-free calculation. are summarized. For further details see Table 15.

	E[MeV]	B(MJ)	E[MeV]	B(MJ)	E[MeV]	B(MJ)
J^{π}, T	H.O.		Woods-Saxon		Experiment	
1^-, 0					9.63	
0	9.2		10.84		12.44	
1	13.79	.06	13.46	.08	13.1	.045±.006
1	17.94	.02	17.39	.008	17.14	.035±.007
0	17.96	.02	17.58	.007	17.3	
0	20.21		19.16		19.	
1	20.8		20.0	.015		
1	23,96	2.94	22.6	3.2	22.3	2.4 (GDR)
1	26.4	1.3	24.9	.612		
2^+, 0	17.39	70.4	21.26	78.6	20.7	50.(GQR)
0	25.03	4.78	25.63	5.01		
3^-, 0	5.07	1411.	6.89	1273.	6.13	1488±70
0					11.6	
0					13.12	
1	13.52	102.	13.28	153.	13.26	
0	16.45	94.2	16.45	147.	15.4	
1	18.93	118.	18.7	174.	19.21	
0	23.46	48.5	23.22	61.2	21.77	

TABLE 16. Unnatural parity states of ^{12}C are summarized. In the first column we have nucleon-nucleon results of RPA calculations with G_{NM}^{II} interaction in the single-particle space of 5 oscillator major shells. In the second column results with inclusion of the Δ-isobar are displayed. 8 major oscillator shells of Δ states are included. The last column shows experimental data.

J^{π}, T	E[MeV]	B(MJ)	E[MeV]	B(MJ)	E[MeV]	B(MJ)
	nucleon-nucleon		delta-nucleon		Experiment	
0^-, 0	16.1		16.1			
(1)					18.4	
1	22.43		22.21			
1^+, 0	11.91	.004	11.91	.003	12.71	.044±.00063
1	16.53	9.60	16.29	8.98	15.11	2.78±.083
2^-, 0					11.83	
0	15.39	16.9	15.39	16.8	13.35	
1	16.5	26.17	16.44	20.17	16.58	
	17.07	39.7	16.97	42.		
1	18.56	581.	18.49	587.	18.3*)	
0	19.8	.005	19.8	.037	19.4*)	
1	21.68	102.	21.58	96.4	(23.05)	
4^-,(1)	17.38	292k	17.32	347k	(18.27)	
(0)	17.55	153k	17.54	100k	(19.56)	

*) see [57]

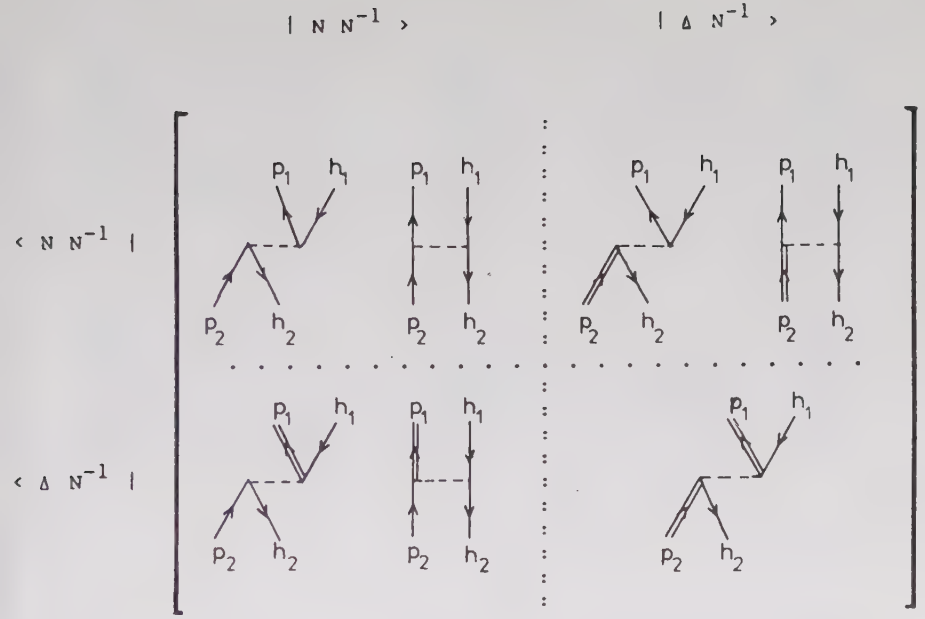

Fig 1a

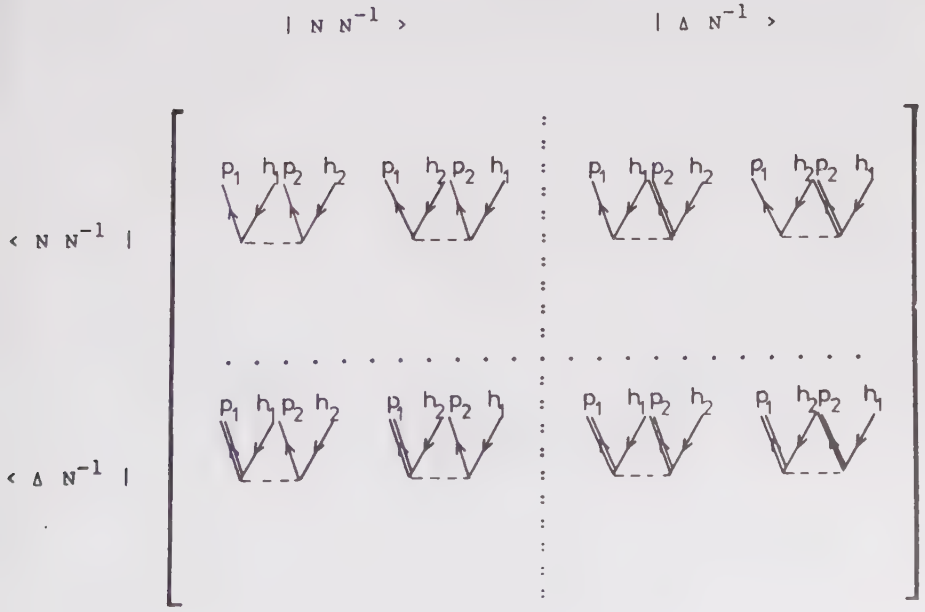

Fig 1b

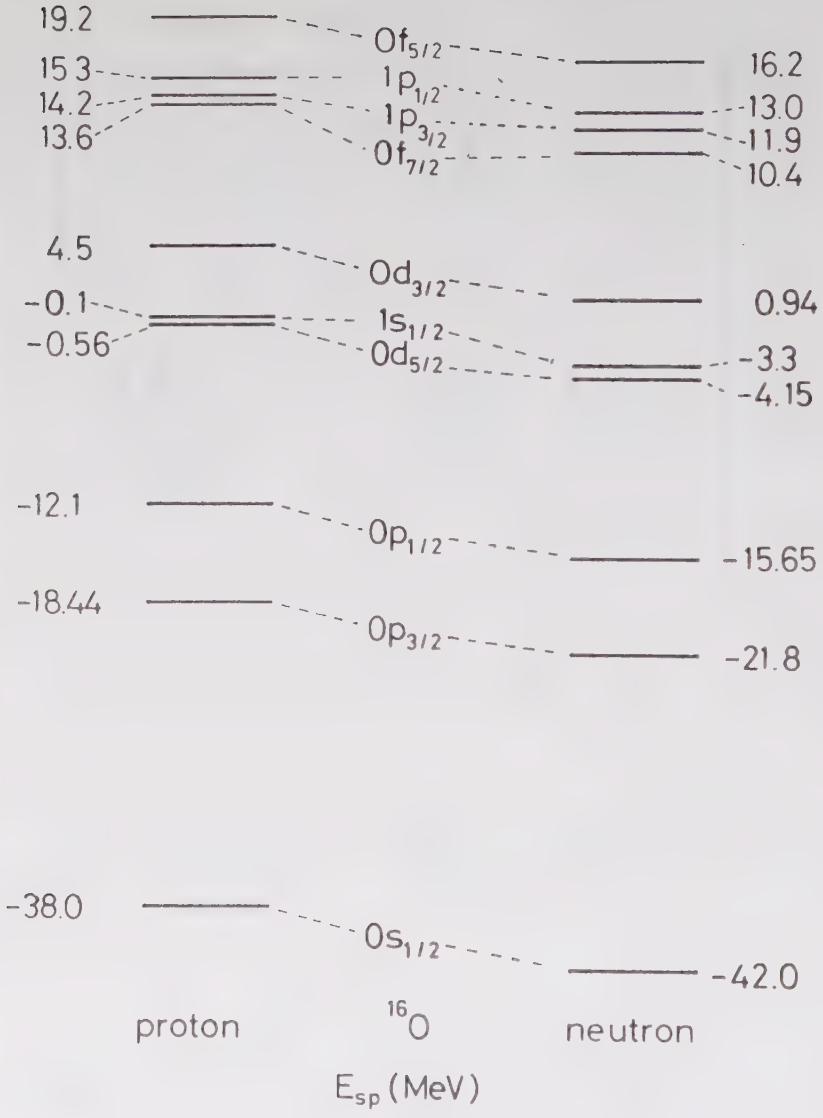
19.2
15.3
14.2
13.6
0f5/2
1p1/2
1p3/2
0f7/2
16.2
13.0
11.9
10.4
4.5
-0.1
-0.56
0d3/2
1s1/2
0d5/2
0.94
-3.3
-4.15
-12.1
-18.44
0p1/2
0p3/2
-15.65
-21.8
-38.0
0s1/2
-42.0
proton
16O
neutron
Esp (MeV)

Fig.2a

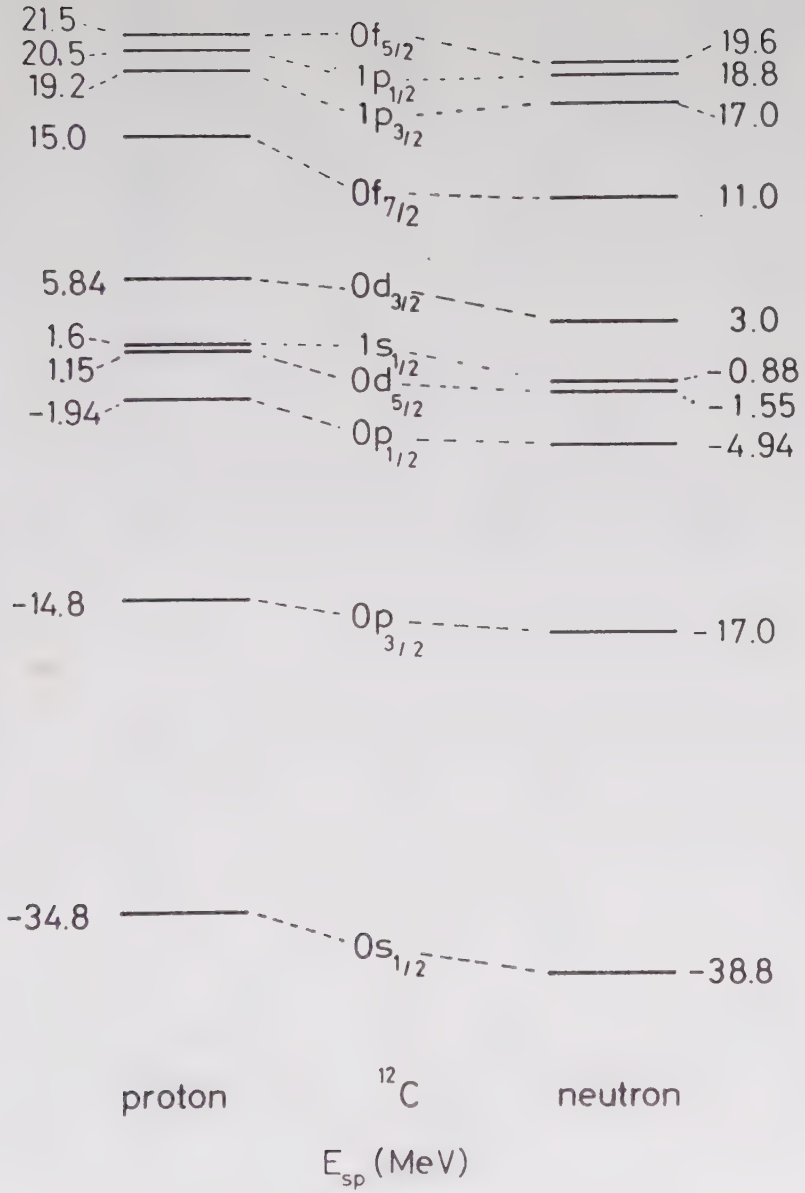
21.5
20.5
19.2
15.0
0f5/2
1p1/2
1p3/2
0f7/2
19.6
18.8
17.0
11.0
5.84
1.6
1.15
-1.94
0d3/2
1s1/2
0d5/2
0p1/2
3.0
-0.88
-1.55
-4.94
-14.8
0p3/2
-17.0
-34.8
0s1/2
-38.8
proton
12C
neutron
Esp (MeV)

Fig.2b

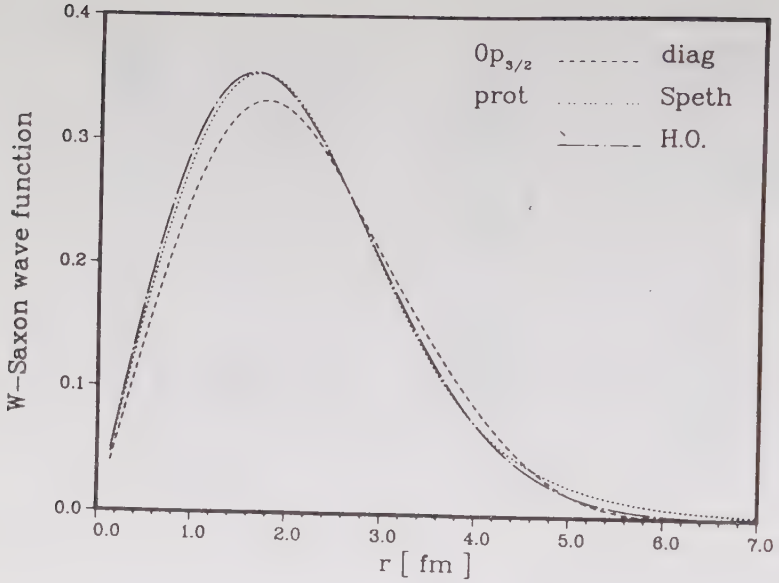
0.4
0.3
0.2
0.1
0.0
W-Saxon wave function
0.0
1.0
2.0
3.0
4.0
5.0
6.0
7.0
r [fm]
0p3/2
prot
diag
Speth
H.O.

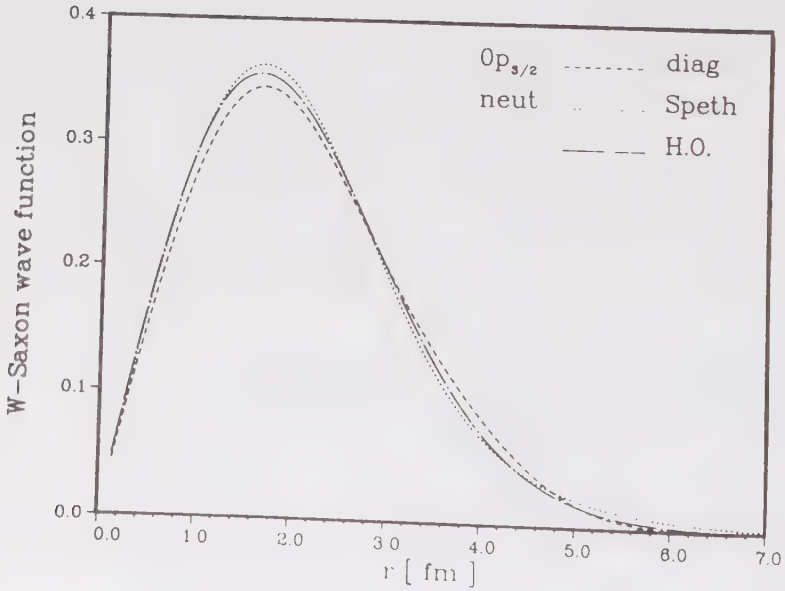
0.4
0.3
0.2
0.1
0.0
W-Saxon wave function
0.0
1.0
2.0
3.0
4.0
5.0
6.0
7.0
r [fm]
0p3/2
neut
diag
Speth
H.O.

Fig.3

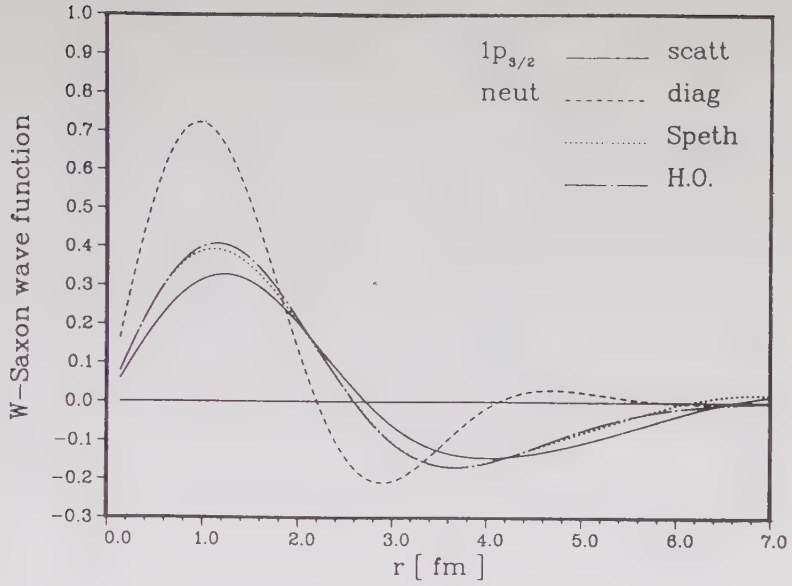
1p3/2
neut
scatt
diag
Speth
H.O.
W-Saxon wave function
r [fm]

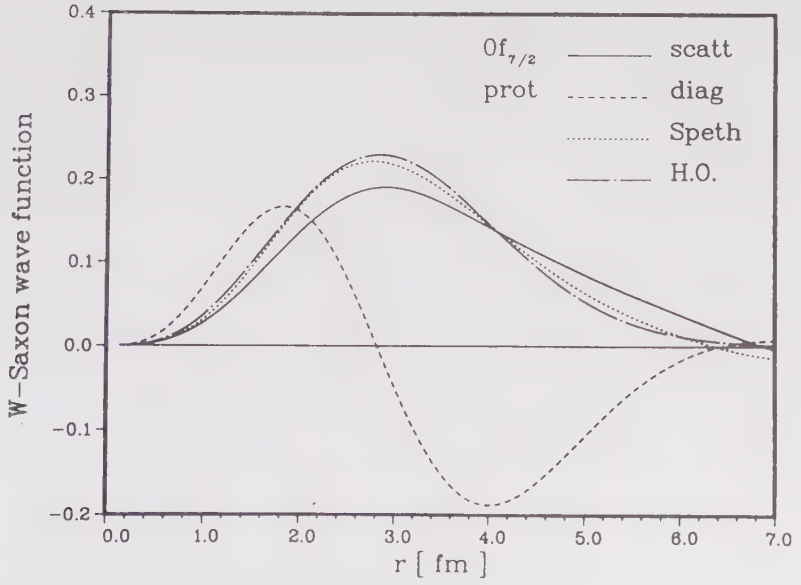
0f7/2
prot
scatt
diag
Speth
H.O.
W-Saxon wave function
r [fm]

Fig.4

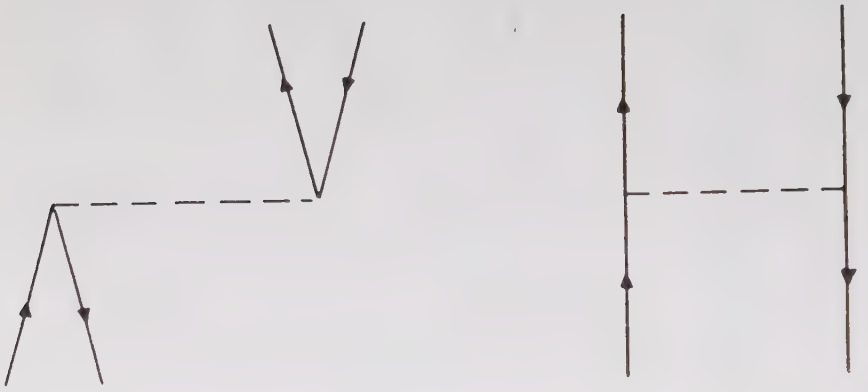

Fig.5

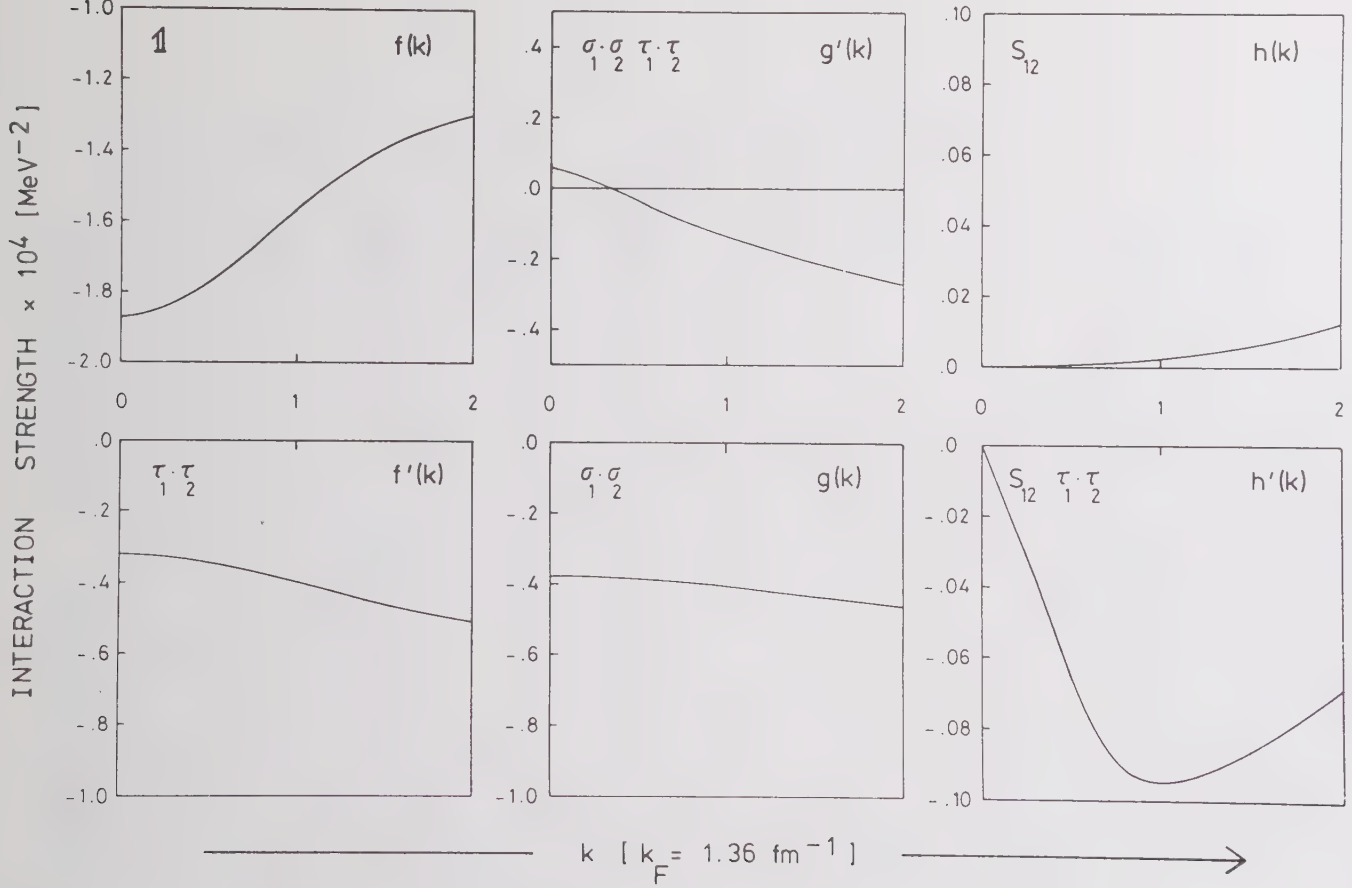
INTERACTION STRENGTH × 10⁴ [MeV⁻²]
1 f(k)
σ·σ τ·τ g'(k)
1 2 1 2
S12 h(k)
τ·τ f'(k)
1 2
σ·σ g(k)
1 2
S12 τ·τ h'(k)
1 2
k [kF = 1.36 fm⁻¹]

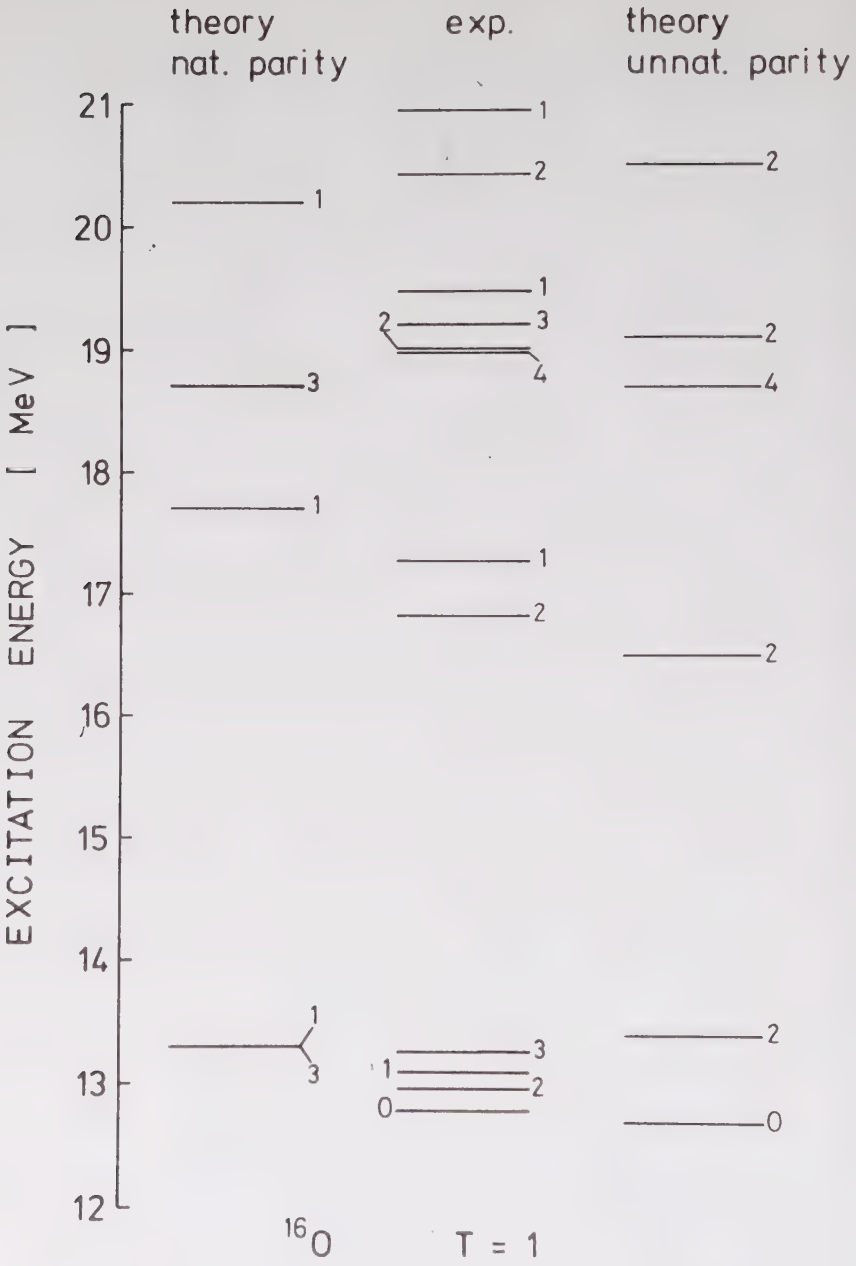
theory
nat. parity
exp.
theory
unnat. parity
EXCITATION ENERGY [MeV]
21
20
19
18
17
16
15
14
13
12
1
1
3
1
1
3
2
1
2
1
2
3
4
1
2
2
2
4
2
2
0
^{16}O
T = 1

Fig.7

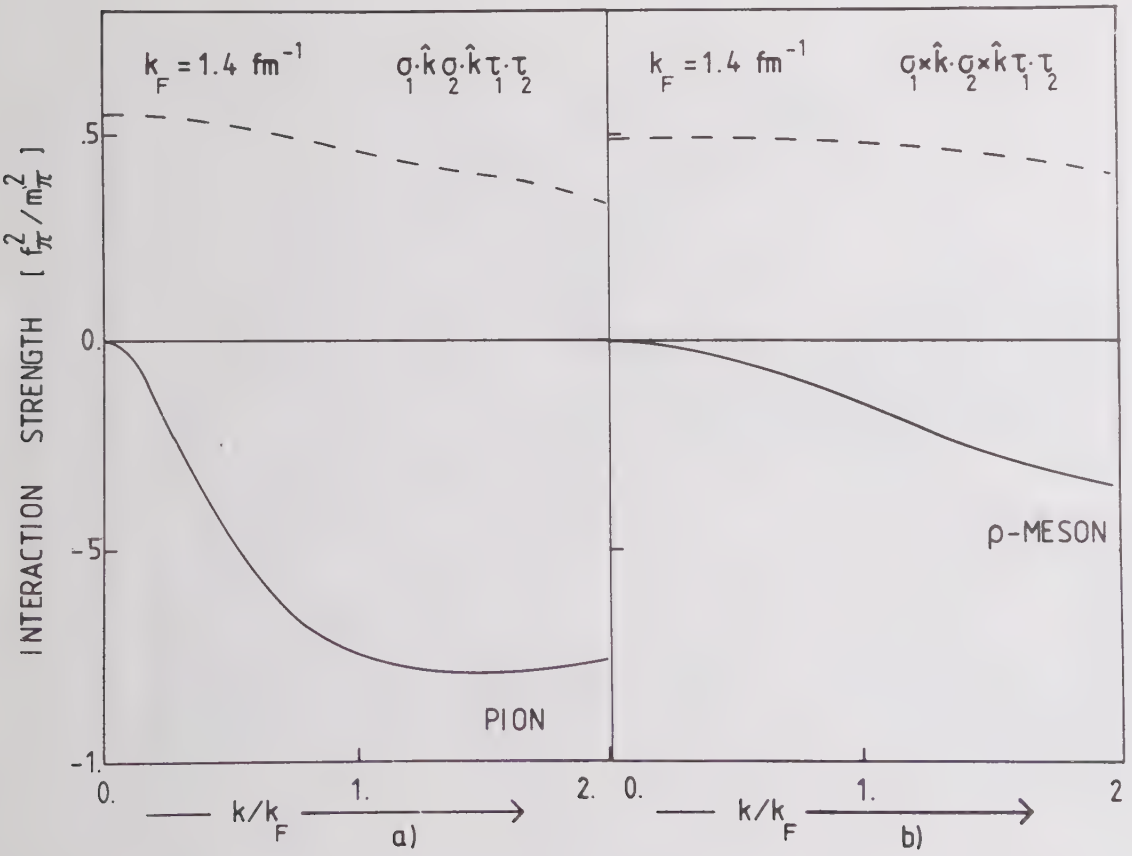
$k_F = 1.4$ fm^{-1}
$\sigma_1 \cdot \hat{k}\, \sigma_2 \cdot \hat{k}\, \tau_1 \cdot \tau_2$
$k_F = 1.4$ fm^{-1}
$\sigma_1 \times \hat{k} \cdot \sigma_2 \times \hat{k}\, \tau_1 \cdot \tau_2$
INTERACTION STRENGTH [f_π^2 / m_π^2]
.5
0.
-5
-1.
PION
ρ-MESON
0.
1.
2.
k/k_F
a)
b)

Fig.8

Fig.9

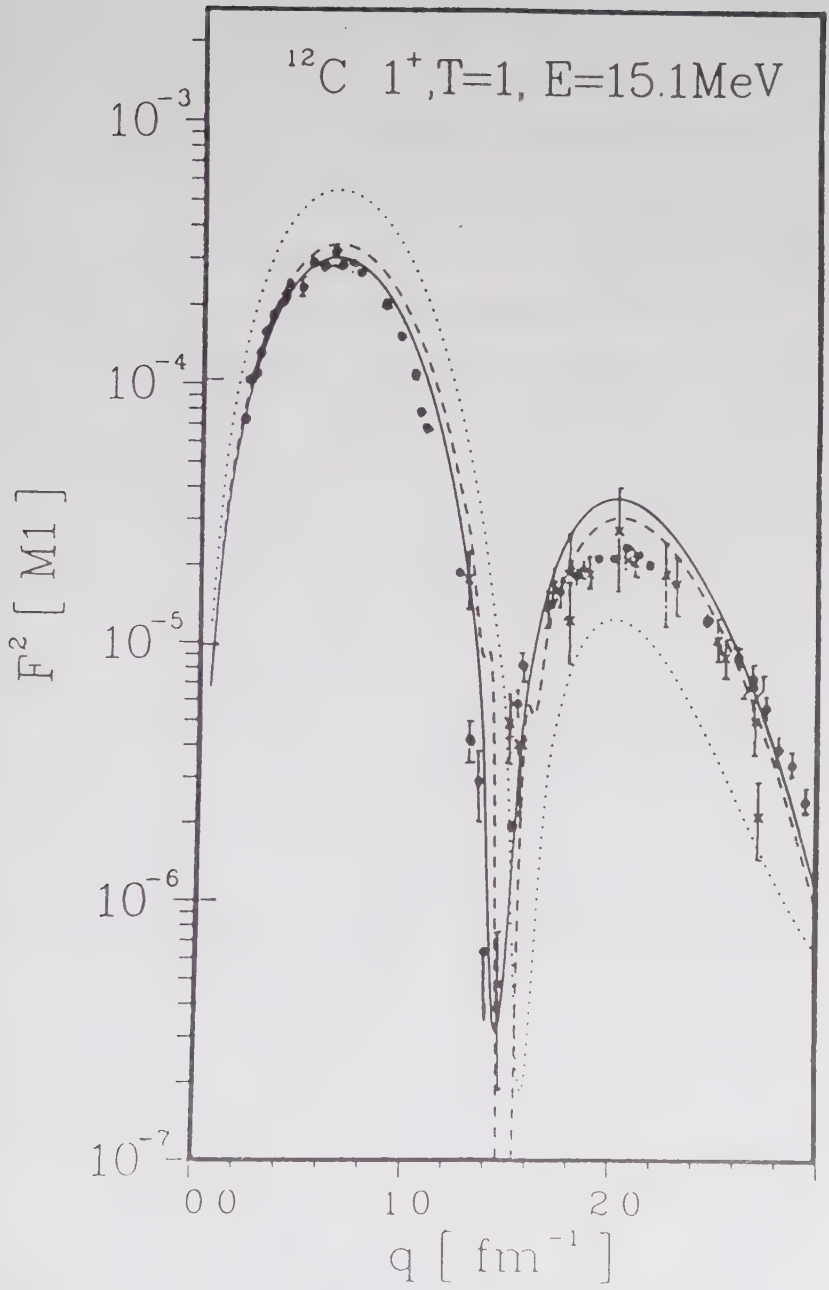

Fig.10

DANKSAGUNG

Ich danke Herrn Prof. Dr. Amand Faessler für die Anregung zu dieser Arbeit sowie für die Anleitungen und fruchtbaren Diskussionen.

Für Zusammenarbeit möchte ich insbesonders den Herren Prof. Dr. H.Müther und Dr. W.Dickhoff danken. Die Diskussion mit den Kollegen und Besuchern des Instituts für Theoretische Physik der Universität Tübingen waren mir eine große Hilfe. Dabei danke ich insbesondere Prof. Dr. Z.Bochnacki, Dr. M.Ploszajczak, Dr. A.Polls, Dr. S.Kuyucak, Dr. M.Nishimura, Dr. F.Fernandez, Dr. S.Toyoda, Dipl. Phys. K.Bräuer, Dipl. Phys. P.K.Rath, Dipl. Phys. G.Lübeck.

Mein herzlichen Dank gilt nochmals Dr. W.Dickhoff für seine Hilfe bei der Korrektur des Manuskripts.

Dem Zentrum für Datenverarbeitung der Universität Tübingen danke ich für die großzügige Überlassung von Rechenzeit.

Dem DAAD (Deutschland) und PAN (Polen) danke ich für die finanzielle Unterstützung der Arbeit.

Ganz besonderer Dank gebührt auch meinen Eltern, meiner Frau und meinen Kindern.

LEBENSLAUF

Ich wurde am 15.06.1956 als Sohn des Ingenieurs Stanislaw Czerski und seiner Frau Jadwiga Czerska, geb. Marcinow geboren.

1971 beendete ich die Grundschule und ging dann bis 1975 in das Gymnasium, jeweils in Krakow, Polen. Anschließend begann ich am 1.10.1975 mein Studium der theoretischen Physik an der Jagiellonian Universität in Krakow.

Während des Studiums heiratete ich am 31.12.1977 Bozena Mastykarz.

Im Februar 1980 legte ich an der Jagiellonian Universität in Krakow mein Diplom ab. Das Thema meiner Diplomarbeit lautet: "Klassifizierung der nicht-relativistischen Grenzfälle der klassischen Elektrodynamik". Die Diplomarbeit wurde von Dr.E.Kapuscik betreut (Institut für Kernphysik in Krakow). Nach dem Studium begann ich am Institut für Kernphysik in Krakow unter Leitung von Prof. Dr. Z.Bochnacki zu arbeiten.

Von Mai 1981 bis Juni 1984 fertigte ich meine Dissertation am Institut für Theoretische Physik der Universität Tübingen unter Anleitung von Prof. Dr. Amand Faessler an.

Meine akademische Lehrer waren die Professoren und Dozenten: Z.Bochnacki, M.Demianski, W.Dittrich, Amand Faessler, E.Kapuscik, P.Kramer, H.Müther, J.Rayski, H.Ruder, E.Schmid, K.W.Schmid, A.Staruszkiewicz, G.Staudt, H.Stumpf, K.Wildermuth, K.Zalewski

Offsetdruck Spengler
Lessingstraße 4 · 7401 Neustetten 1
Telefon (0 74 72) 2 21 45